RESEARCH ARTICLE

A conserved glutamate residue in RPM1-interacting protein4 is ADP-ribosylated by *Pseudomonas* effector AvrRpm2 to activate RPM1-mediated response

Minsoo Yoon[1*], Martin Middleditch[2], Erik Rikkerink[1]

[1]The New Zealand Institute for Plant and Food Research, Auckland, New Zealand

[2]University of Auckland, Auckland, New Zealand

*Correspondence: Minsoo Yoon (minsoo.yoon@plantandfood.co.nz)

Short title: Posttranslational modification of host protein RIN4 by pathogen effector AvrRpm2$_{Psa}$

One sentence summary: A conserved glutamate residue (E156) in the C-NOI domain of RPM1-interacting protein4 is ADP-ribosylated by *Pseudomonas* effector AvrRpm2 to activate RPM1-mediated defence response, independently of phosphorylation at T166.

ABSTRACT

Gram-negative bacterial plant pathogens directly inject effectors into their hosts to hijack and manipulate metabolism, eluding the frontier surveillance at the cell surface. The effector AvrRpm1$_{Pma}$ from *Pseudomonas syringae* pv. *maculicola* functions as an ADP-ribosyl transferase, modifying RPM1-interacting protein4 (RIN4), leading to the activation of Arabidopsis resistance protein RPM1. We identified the ADP-ribosyl transferase activity of another bacterial effector AvrRpm2$_{Psa}$ from *Pseudomonas syringae* pv. *actinidiae* via infection using a *Pseudomonas syringae* pv. *tomato* strain following Agrobacterium-mediated transient expression of RIN4 in *N. benthamiana*. We conducted mutational analysis in combination with mass spectrometry to genetically locate the modified residue. We show that a conserved glutamate residue (E156) of AtRIN4 is the target site for AvrRpm2$_{Psa}$ by demonstrating the modified AtRIN4 with E156A substitution is no longer ADP-ribosylated. Accordingly, naturally occurring soybean and snap bean RIN4 homologs with no glutamate at the positions corresponding to the E156 of AtRIN4 are not ADP-ribosylated by AvrRpm2$_{Psa}$. In contrast with another effector AvrB, modifications of potential phosphorylation sites including T166 in AtRIN4 affected neither ADP-ribosylation nor RPM1 activation by AvrRpm2$_{Psa}$. This study suggests that separate biochemical reactions by different pathogen effectors may trigger the activation of the same resistance protein through distinct modifications of RIN4.

INTRODUCTION

Bacterial plant pathogens such as *Pseudomonas*, *Ralstonia*, *Xanthomonas*, and *Erwinia* can cause a variety of diseases in economically important crop plants (Mansfield et al., 2012). Over long periods of co-existence, both hosts and pathogens have evolved features to combat each other (Bent and Mackey, 2007). At the battle frontier on the cell surface (Malinovsky et al., 2014), various pattern recognition receptors (Macho and Zipfel, 2015; Kong et al., 2021) sense the presence of a pathogen by recognising pathogen-associated molecular patterns (PAMPs) (Ingle et al., 2006), which are signature molecules of pathogens, for example, flagellin or lipopolysaccharides (Felix et al., 1999; Yu et al., 2021), also known as microbe-associated molecular patterns (Ausubel, 2005). Evading host surveillance at the cell wall, pathogens directly inject bacterial proteins into plant cells via a specialised delivery apparatus

known as the type III secretion system (T3SS) (Coombes, 2009; Buttner, 2012; Puhar and Sansonetti, 2014). Successful proliferation of pathogens depends on secreted proteins known as type III effectors (T3Es) (Alfano and Collmer, 2004; Block et al., 2008; Block and Alfano, 2011).

Unlike PAMPs, which are fragments from bacterial molecules often conserved for essential microbial life, effectors are specially designed tools for aggressive host colonisation. Effectors may have specific enzymatic activities such as phosphorylation, ubiquitination, acetylation, proteolysis, or ADP-ribosylation (Ribet and Cossart, 2010). Once translocated inside plant cells, T3Es manipulate essential cellular processes to promote pathogen virulence and neutralize defence responses. However, this effector injection strategy is counterbalanced by another layer of host responses orchestrated by resistance (R) genes (Belkhadir et al., 2004; DeYoung and Innes, 2006). Once activated, an R gene may lead to strong defence responses including a hypersensitive responses (HR), often manifested by localised cell death to minimise the spread of infection (Guo et al., 2009; Lindeberg et al., 2012). The encoded R proteins may recognise translocated pathogen effectors via direct physical association or indirectly through perception of the enzymatic activities required for effector function (Dangl and Jones, 2001; van der Hoorn and Kamoun, 2008).

The T3E AvrRpm1$_{Pma}$ from the phytopathogen *Pseudomonas syringae* pv. *maculicola* (Pma) triggers activation of Arabidopsis resistance protein RPM1 (Mackey et al., 2002). The RPM1-mediated defence response is closely linked to the modification of RPM1-interacting protein4 (RIN4) (Chung et al., 2011; Liu et al., 2011; Xu et al., 2017). All events involved in the sequence of interactions, translocation of the bacterial effector into the host via T3SS, posttranslational modification of the host protein RIN4 (Kim et al., 2005), and the activation of resistance protein RPM1 for eventual defence response, are critical for the progression of resistance or disease (Dodds and Rathjen, 2010; Cui et al., 2015). In particular, the ubiquitous plant protein RIN4, a probable regulator of plant immunity (Rikkerink, 2018; Toruno et al., 2019), is a target for multiple effectors (Mackey et al., 2003; Chung et al., 2014; Zhao et al., 2021). However, the physiological or functional role of RIN4 is not clearly defined despite the wide distribution of this protein among plants including mosses (Afzal et al., 2013). The bacterial effector AvrRpm1$_{Pma}$ functions as an ADP-ribosyl transferase, modifying RIN4 (Cherkis et al., 2012; Redditt et al., 2019). The target residues of AvrRpm1$_{Pma}$ were identified via mass spectrometry analysis following Agrobacterium-mediated transient expression of a

soybean RIN4 homolog GmRIN4b in *N. benthamiana*. It was reported that a D153 substitution in the C-terminal nitrate-induced (NOI) domain of AtRIN4 inhibited phosphorylation of T166 and eventually inhibited the RPM1-mediated restriction of pathogen growth, supposedly by blocking ADP-ribosylation at this position (Redditt et al., 2019). However, it is still not clear how the ADP-ribosyl transferase activity of AvrRpm1$_{Pma}$, the phosphorylation of the RIN4, and the activation of RPM1 are interconnected to initiate the host response.

Kiwifruit canker disease (Vanneste et al., 2013; Donati et al., 2020) caused by *Pseudomonas syringae* pv. *actinidiae* (Psa) was first reported in Japan (Serizawa et al., 1989) followed by China, Korea, Italy, and then it rapidly spread around the world (Fang et al., 1990; Koh et al., 1994; Scortichini, 1994; McCann et al., 2017). Psa strains collectively have about 50 T3E loci (McCann et al., 2013). While most Psa effectors have not been functionally characterised, some effectors show varying degrees of sequence similarities with previously characterised effectors from other related species such as *Pseudomonas syringae* pv. *tomato* (HopQ1$_{Pto}$ or HopF2$_{Pto}$), *Pseudomonas syringae* pv. *syringae* (AvrRpm1$_{Psy}$ or HopZ3$_{Psy}$), or *Pseudomonas syringae* pv. *maculicola* (AvrRpm1$_{Pma}$), raising the possibility that some effector functions are conserved at least partially, even though the pathogens have different hosts (Cunnac et al., 2009; Baltrus et al., 2011; Dharmaraj, 2018). In particular, most Psa strains have AvrRpm2$_{Psa}$ loci, having about 50% protein sequence identity with AvrRpm1$_{Pma}$, in various allelic forms (McCann et al., 2013; Fujikawa and Sawada, 2016), suggesting frequent selection and counter-selection during host-pathogen interactions.

ADP-ribosylation is a reversible posttranslational modification (PTM) catalysed by a group of enzymes known as ADP-ribosyl transferases (ARTs) (Hottiger et al., 2010). They are sub-classified based on conserved motifs of either H-Y-E (Diphteria toxin or DTX family) or R-S-E (Cholera toxin or CTX family) in the catalytic domains (Simon et al., 2014; Mikolcevic et al., 2021). Recent studies show that ADP-ribosylation is exploited both by bacteria to achieve stealth attacks on their hosts and by plants to launch effective defence (Feng et al., 2016). Mass-spectrometry analysis has become the main analytical tool for identifying PTMs (Doll and Burlingame, 2015). However, there is a major technical limitation of mass spectrometry analysis in locating target sites of ADP-ribosylation. Due to the lability of the bond between the ADP-ribose moiety and the side-chain of the modified amino acid during fragmentation, compared with the relatively stable peptide bonds between amino acid

residues, generating all possible combinations of fragment ions retaining the ADP-ribose moiety is often difficult (Rosenthal et al., 2015; Hendriks et al., 2019). Combined with the fact that many different amino acid residues can be modified (Cohen and Chang, 2018), accurate localization of ADP-ribosylation can be analytically challenging.

Here we report the identification of the target residue in RIN4 for the bacterial effector AvrRpm2$_{Psa}$, which also functions as an ADP-ribosyl transferase. To complement the limitation of mass spectrometry, which eventually could not generate all necessary combinations of fragment ions required for unambiguous identification of the modified residue, we conducted mutational analysis to genetically identify the target. To preclude potentially aberrant activities of the bacterial effectors expressed *in planta*, we delivered the bacterial protein via infection using a Pto strain instead of Agrobacterium-mediated transient expression. With the combination of mass spectrometry, mutational analysis, and infection delivery, we located a conserved glutamate residue (E156) in AtRIN4 as the target for the AvrRpm2$_{Psa}$ activity. We found matching polymorphisms at positions corresponding to E156 of AtRIN4 with the RPM1-mediated HR phenotypes among naturally occurring RIN4 homologs of soybean (*Glycine max*), snap bean (*Phaseolus vulgaris*) and apple (*Malus* x *domestica*), demonstrating that the RIN4 target site for this effector is conserved across plant species.

RESULTS AND DISCUSSION

AvrRpm2$_{Psa}$ functions as an ADP-ribosyl transferase modifying RIN4

Sequence alignment with known ADP-ribosyl transferases such as diphtheria toxin or Exotoxin A (Exo T) suggested that AvrRpm1$_{Pma}$ has three conserved residues (H63, Y122, and D185) in catalytic domains (Cherkis et al., 2012). It was later biochemically shown that AvrRpm1$_{Pma}$ functions as an ADP-ribosyl transferase to modify RIN4, leading to the activation of Arabidopsis resistance protein RPM1 (Redditt et al., 2019). AvrRpm1$_{Pma}$ has the H-Y-D motif in potential catalytic domains and therefore may be classified as a member of the DTX family along with *Pseudomonas aeruginosa* Exo T, a T3E required for full virulence in animal model of an acute pneumonia, which has the H-Y-E motif (Garrity-Ryan et al., 2004). While AvrRpm2$_{Psa}$ shares about 50% protein sequence with AvrRpm1$_{Pma}$, the

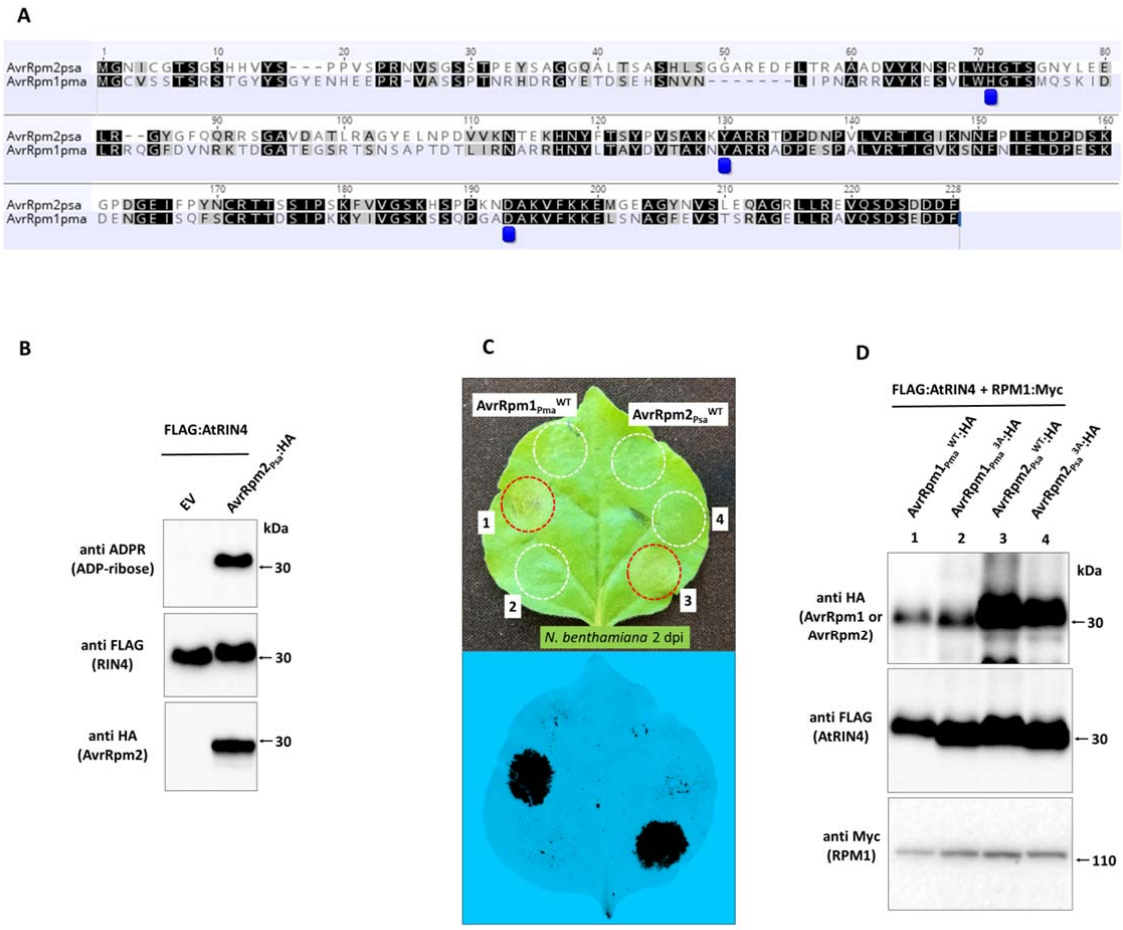

Figure 1. Transient co-expression of AtRIN4 and AvrRpm2$_{Psa}$ (biovar 5) in *N. benthamiana* via Agrobacterium. **A.** Sequence alignment of AvrRpm2$_{Psa}$ and AvrRpm1$_{Pma}$. The residues (H63, Y122, and D185) in the conserved H-Y-D motif of AvrRpm1$_{Pma}$, proposed previously (Cherkis et al., 2012), are marked with blue labels. The corresponding residues in the H-Y-D motif of AvrRpm2$_{Psa}$ are H68, Y125, and D188. **B.** Western blot analysis demonstrating the ADP-ribosyl transferase activity of AvrRpm2$_{Psa}$. Proteins were extracted from *N. benthamiana* leaves co-expressing AvrRpm2$_{Psa}$:HA and FLAG:AtRIN4 via Agrobacterium at 2 d post infiltration. ADP-ribosylated proteins were detected using the anti ADPR binding reagent. FLAG:RIN4 and AvrRpm2$_{Psa}$:HA were detected using corresponding antibodies. **C**. RPM1-mediated HR (hypersensitive response) assay. An *N. benthamiana* leaf co-expressing FLAG:AtRIN4 and RPM1:Myc with either AvrRpm1$_{Pma}$ or AvrRpm1$_{Pma}$ in different combinations (1: AvrRpm1$_{Pma}^{WT}$:HA (wild type); 2: AvrRpm1$_{Pma}^{3A}$ (triple substitutions: H63A, Y122A, D185A); 3: AvrRpm2$_{Psa}^{WT}$:HA (wild type); 4: AvrRpm2$_{Psa}^{3A}$ (triple substitutions: H68A, Y125A, D188A) delivered via Agrobacterium. Red circles denote HR and white circles denote no HR. The fluorescence of the same leaf monitored under a 488 nm tray in the ChemiDoc™ is also shown (bottom). Images were taken 2 d post Agrobacterium infiltration. **D**. Western blot analysis using proteins extracted from the corresponding areas of the leaf used in **C** 2 d post Agrobacterium injection.

proposed three critical residues (H-Y-D) in AvrRpm1$_{Pma}$ are also conserved in AvrRpm2$_{Psa}$ (Figure 1A).

We tested AvrRpm2$_{Psa}$ for its function as an ADP-ribosyl transferase. Proteins were extracted from *N. benthamiana* leaves transiently co-expressing AtRIN4 and AvrRpm2$_{Psa}$ via Agrobacterium. When Western blot analysis was performed using anti-ADPR binding reagent to detect ADP-ribosylated proteins, the AtRIN4 protein band was detected, demonstrating that AvrRpm2$_{Psa}$ functions as an ADP-ribosyl transferase modifying AtRIN4 (Figure 1B). When AvrRpm2$_{Psa}$ was co-expressed with AtRIN4 and RPM1 via

Agrobacterium in *N. benthamiana*, an RPM1-mediated HR was observed (Figure 1C, top). When the fluorescence from the infiltrated leaf was monitored in the ChemiDoc™ with trays specific for 488nm, loss of green specks due to cell collapse were more clearly visible (Figure 1C, bottom) (Yoon and Rikkerink, 2020). As reported previously, modifications of the three sites (H-Y-D) in AvrRpm1$_{Pma}$ (AvrRpm1$_{Pma}^{3A}$ with triple substitutions at H63A, Y122A, and D185A) resulted in the loss of the RPM1-mediated HR (Cherkis et al., 2012; Redditt et al., 2019). Modifications of the three corresponding residues in AvrRpm2$_{Psa}$ (AvrRpm2$_{Psa}^{3A}$ with the corresponding triple substitutions at H68A, Y125A, and D188A) similarly resulted in the loss of the RPM1-mediated response, demonstrating the importance of the H-Y-D motif in the two bacterial effectors. Western blot analysis (Figure 1D) showed that the modified proteins accumulated similarly when compared with their corresponding wild type proteins, suggesting the observed differences in the HR are due to the changes in their biochemical activities, not in their accumulation.

RIN4 is a widely-distributed plant protein capable of physically associating with other proteins, making multi-protein complexes (Sun et al., 2014; Rikkerink, 2018; Ray et al., 2019). There are several bacterial effectors known to physically associate with RIN4, including AvrB (Lee et al., 2004), AvrRpm1$_{Pma}$ (Mackey et al., 2002), AvrRpm1$_{Psa}$ (Yoon and Rikkerink, 2020), HopF2$_{Pto}$ (Wilton et al., 2010), and HopZ3$_{Psy}$ (Lee et al., 2015b), suggesting frequent participation of RIN4 in pathogen-plant interactions. To test the protein association with RIN4, AvrRpm2$_{Psa}$ with an epitope tag (AvrRpm2$_{Psa}$:HA) was co-expressed with AtRIN4, tagged with a different epitope (FLAG:AtRIN4), in *N. benthamiana* via Agrobacterium. Both proteins were detected in the Western blot analysis with corresponding antibodies (Figure 2A). Proteins were immunoprecipitated with anti HA-conjugated magnetic beads to isolate AvrRpm2$_{Psa}$. Western blot analysis showed that AtRIN4 was co-precipitated with AvrRpm2$_{Psa}$, showing AtRIN4 physically associated with AvrRpm2$_{Psa}$ (Figure 2A, third lane, Co-IP panel). There was no comparable AtRIN4 co-precipitated with the empty vector (EV) or HA-tagged AtRIN4 (HA:AtRIN4), showing the protein-protein interaction between AvrRpm2$_{Psa}$ and AtRIN4 was specific. AtRIN4 co-expressed with AvrRpm2$_{Psa}$ showed a change in mobility during electrophoresis. As shown in the Western blot analysis, AtRIN4 co-expressed with AvrRpm2$_{Psa}$ (Figure 2B, even-numbered) showed a consistently slower migration in SDS-PAGE compared with those from leaves without AvrRpm2$_{Psa}$ (odd-

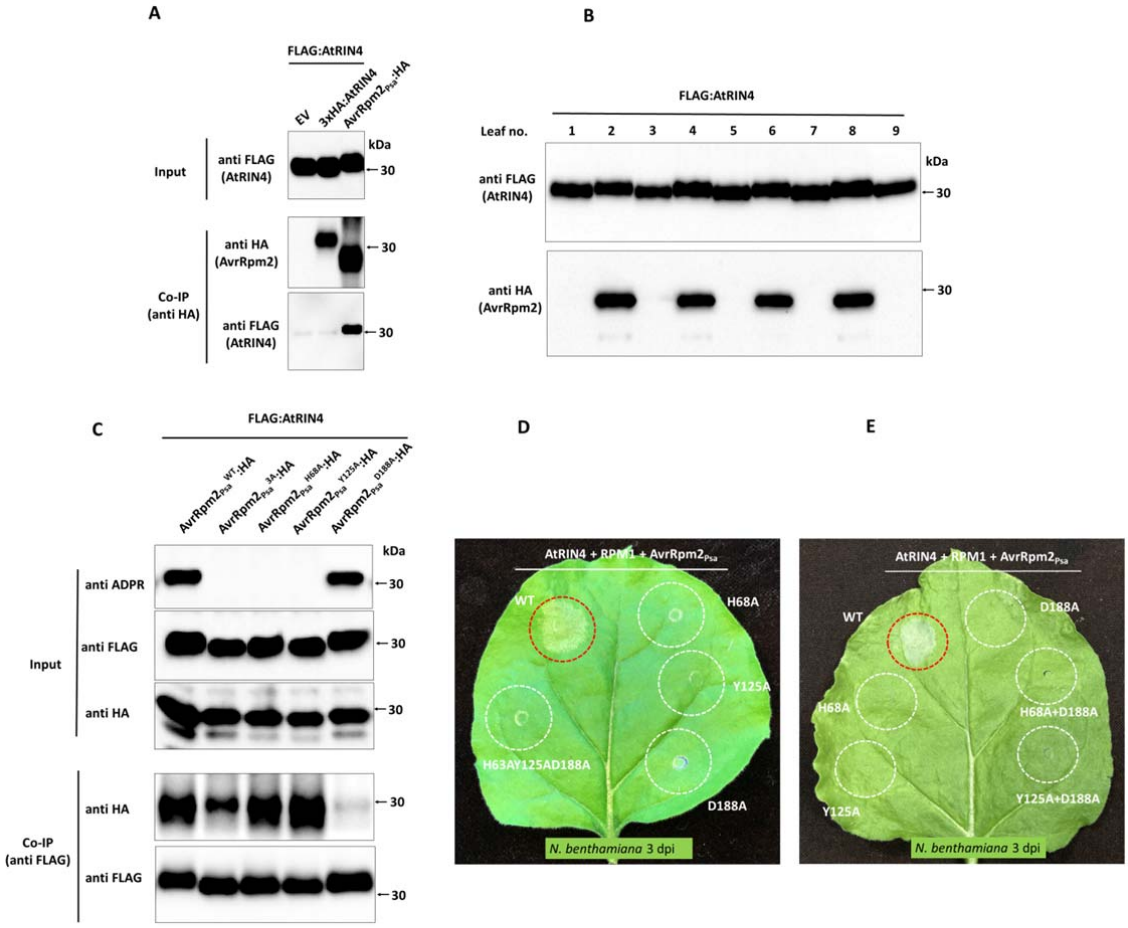

Figure 2. Western blot analysis of AtRIN4 transiently co-expressed with AvrRpm2$_{Psa}$ in *N. benthamiana* via Agrobacterium. **A**. Proteins were extracted from *N. benthamiana* leaves co-expressing FLAG:AtRIN4 with either Empty vector (lane 1), HA:AtRIN4 (lane 2), or AvrRpm2$_{Psa}$:HA (lane 3) via Agrobacterium. Protein extracts were immunoprecipitated using anti HA magnetic beads. Precipitated proteins were probed with corresponding antibodies. **B**. Western blot analysis showed the ADP-ribosylated AtRIN4 migrated more slowly compared with unmodified AtRIN4 during SDS-PAGE. Protein extracts from *N. benthamiana* leaves co-expressing FLAG:AtRIN4 with AvrRpm2$_{Psa}$:HA (even-numbered) or expressing only FLAG:AtRIN4 (odd-numbered) were probed. **C**. Western blot analysis of different AvrRpm2$_{Psa}$ alelles (AvrRpm2$_{Psa}^{WT}$, AvrRpm2$_{Psa}^{H68A}$, AvrRpm2$_{Psa}^{Y125A}$, AvrRpm2$_{Psa}^{H188A}$, and AvrRpm2$_{Psa}^{3A}$) co-expressed with AtRIN4 via Agrobacterium (Input panel). For Co-IP of modified AvrRpm2 with AtRIN4 (Co-IP panels), protein extracts were precipitated using anti FLAG magnetic beads to isolate FLAG:AtRIN4. Precipitated proteins were probed using corresponding antibodies. **D.** Modified AvrRpm2 alleles (AvrRpm2$_{Psa}^{H68A}$, AvrRpm2$_{Psa}^{Y125A}$, and AvrRpm2$_{Psa}^{D188A}$) were co-expressed with RPM1 and AtRIN4 on an *N. benthamiana* leaf to assess the corresponding RPM1-mediated HR. **E.** Combinations of modified AvrRpm2 alleles (AvrRpm2$_{Psa}^{D188A}$ with AvrRpm2$_{Psa}^{H68A}$ and AvrRpm2$_{Psa}^{D188A}$ with AvrRpm2$_{Psa}^{Y125A}$) were co-expressed with RPM1 and AtRIN4 on an *N. benthamiana* leaf. Red circles denote HR and white circles denote no HR. Images were taken at 3 d post Agrobacterium injection (**D** and **E**)

numbered), suggesting a change in the structure of the ADP-ribosylated RIN4 compared with the unmodified RIN4. Similar changes in the mobility of RIN4 during electrophoresis were reported previously with co-expressed AvrRpm1$_{Pma}$ (Redditt et al., 2019).

Modifications in the H-Y-D motif of AvrRpm2$_{Psa}$ affect activity or affinity

Modified AvrRpm1$_{Pma}$ with either H63A, Y122A, or D185A substitution resulted in significant loss in the RPM1-mediated restriction of pathogen growth in Arabidopsis (Cherkis

et al., 2012). We made corresponding substitutions of H68A, Y125A, and D188A in the H-Y-D motif of AvrRpm2$_{Psa}$ to create AvrRpm2$_{Psa}^{H68A}$, AvrRpm2$_{Psa}^{Y128A}$, and AvrRpm2$_{Psa}^{D188A}$ to analyse their activities as well as their abilities to physically associate with AtRIN4. Proteins were extracted from *N. benthmiana* leaves co-expressing the modified AvrRpm2$_{Psa}$ with AtRIN4 via Agrobacterium. Western blot analysis showed that AvrRpm2$_{Psa}^{H68A}$, AvrRpm2$_{Psa}^{Y125A}$ lost the catalytic activity to modify AtRIN4 while AvrRpm2$_{Psa}^{D188A}$ retained the activity (Figure 2C, anti ADPR in Input panel). In contrast, Co-IP analysis showed that AvrRpm2$_{Psa}^{D188A}$ lost the physical association with AtRIN4 while AvrRpm2$_{Psa}^{H68A}$ and AvrRpm2$_{Psa}^{Y125A}$ still associated with RIN4 (Figure 2C, anti HA in Co-IP panel). When the modified AvrRpm2$_{Psa}$ proteins were co-expressed with AtRIN4 and RPM1 in *N. benthamiana* via Agrobacterium, all three individual substitutions (H68A, Y125A, or D188A) resulted in the loss of the corresponding RPM1-mediated HR (Fig 2D). Therefore, for the bacterial effector to activate RPM1, the ability to physically associate with RIN4 is also required in addition to the functional ability to modify RIN4. Next, we co-expressed AvrRpm2$_{Psa}^{H68A}$ and AvrRpm2$_{Psa}^{D188A}$ in *N. benthamiana* with AtRIN4 and RPM1 to see whether RPM1 can be activated by the catalytic activity of AvrRpm2$_{Psa}^{D188A}$ to modify AtRIN4 while the protein association with AtRIN4 can be separately provided by AvrRpm2$_{Psa}^{H68A}$. We also similarly tested the combined expression of AvrRpm2$_{Psa}^{Y125A}$ with AvrRpm2$_{Psa}^{D188A}$. Neither combination triggered the corresponding RPM1-mediated HR in *N. benthamiana*, demonstrating that the protein association with AtRIN4 and the catalytic activity to modify AtRIN4 cannot be separately provided to activate RPM1 (Figure 2E).

Mass spectrometry analysis of AtRIN4 co-expressed with AvrRpm1$_{Pma}$ in *N. benthamiana* via Agrobacterium

Previously, two residues N12 and D185 in GmRIN4b were identified as the target sites for AvrRpm1$_{Pma}$ (Redditt et al., 2019). To locate the target residue(s) in AtRIN4 for the AvrRpm2$_{Psa}$ activity, we adopted a similar approach. As a preliminary control analysis we first analysed the ADP-ribosylation of AtRIN4 with co-expressed AvrRpm1$_{Pma}$. An N-FLAG tagged AtRIN4 (FLAG:AtRIN4) was co-expressed with AvrRpm1$_{Pma}$ in *N. benthamiana* via Agrobacterium and isolated by immunoprecipitation using anti FLAG-conjugated magnetic beads (Figure S1A). The protein band corresponding to AtRIN4 was excised from the gel and confirmed by Western blot analysis (Figure S1B). After LC-MS/MS analysis of the excised

AtRIN4 protein band, we detected ADP-ribosylated peptides from the two nitrate-induced (NOI) domains. Available fragment evidence suggested that two residues (N157 and N158) in the C-NOI domain and the corresponding two residues (E16 and N17) in the N-NOI domian were likely to be ADP-ribosylated. Not every possible combination of fragment ions were recovered, and most ADP-ribose moieties identified were in degraded forms such as phospho-ribose or ribose, suggesting the lability of the ADP-ribose moiety during fragmentation. Examples of fragmentation data are shown in Figure S1C and Figure S1D.

The target sites of AvrRpm1$_{Pma}$ previously identified in GmRIN4b (N12 and D185) correspond to N11 and D153 in AtRIN4, respectively (Redditt et al., 2019), which are clearly distinct from the target residues we identified (E16, N17, N157, N158) by directly analysing AtRIN4. In an effort to resolve the discrepancy, we created modified RIN4 alleles by replacing target sites identified by both analyses with alanine to prevent modification on these sites. GmRIN4^{N12AD185A} and corresponding AtRIN4^{N11AD153A} were created based on the earlier analysis of GmRIN4b, and AtRIN4^{E16AN17AN157AN158A} was created based on our mass spectrometry analysis. Proteins were extracted from *N. benthamiana* leaves co-expressing AvrRpm1$_{Pma}$ with the modified RIN4 proteins via Agrobacterium. Western blot analysis showed that all of the modified RIN4 proteins were still ADP-ribosylated (Figure S2A and Figure S2B) and also activated RPM1 (Figure S2C). Even when further modification with all six residues (N11, E16, N17, D153, N157, and N158) collectively identified by both analyses were replaced, the modified protein (AtRIN4^{E11AE16AN17AD153AN157AN158A}) was still ADP-ribosylated when co-expressed with AvrRpm1$_{Pma}$ (Figure S2B).

The absence of the target residues identified by the mass spectrometry analyses affected neither the ADP-ribosylation by AvrRpm1$_{Pma}$ nor the activation of RPM1. Therefore, the identification of target residues may have been incorrect with the wrong residues identified due to the hyperactivity of the bacterial effector expressed *in planta* via Agrobacterium, or the mass spectrometry analyses were incomplete with other target residues still unidentified due to the lability of the bonds between ADP-ribose moieties and amino acids side chains. Another possibility is that there are preferences for AvrRpm1$_{Pma}$ among multiple residues and that some sites are modified only when more preferred sites are absent. We similarly analysed AtRIN4 co-expressed with AvrRpm2$_{Psa}$ in *N. benthamiana* via Agrobacterium. Compared with AvrRpm1$_{Pma}$, fewer ADP-ribosylated peptides were identified with AvrRpm2$_{Psa}$ (Figure S3A) and the intensities of fragment ions were lower in the MS/MS

spectra (Figure S3B). Available fragmentation spectra suggested that the target site was likely to be in the C-NOI domain. However, not all combinations of fragment ions were generated and unambiguous identification of the target site was difficult.

Bacterial effectors can be efficiently delivered into *N. benthamiana* by Pto DC3000Q$^-$

Even though a few modified residues were identified, we still could not biochemically verify them as real targets (Figure S2). In particular, it cannot be ruled out that the bacterial effectors expressed *in planta* via Agrobacterium may not have identical properties to the secreted effector via T3SS during an infection. Therefore, we compared the activities of T3SS-delivered effectors with those of the effectors expressed *in planta* via Agrobacterium. Previously, we developed a pathogen assay system in *N. benthamiana* by co-injecting Agrobacterium and the Pto DC3000 strain without hopQ1 (Wei et al., 2007), Pto DC3000Q$^-$, simultaneously (Yoon and Rikkerink 2020). At low bacterial concentrations (OD_{600}=0.00001 to 0.0001 for Pto DC3000Q$^-$ and OD_{600}=0.01 to 0.04 for Agrobacterium), Agrobacterium and Pto DC3000Q$^-$ did not interfere with each other, facilitating bacterial pathogen growth assays. Buscaill et al (2021) reported a similar disease assay based on sequential infection of Pto DC3000Q$^-$ following Agrobacterium-mediated transient expression in *N. benthamiana* (Buscaill et al., 2021).

By adopting a similar sequential approach, we first transiently expressed RIN4 in *N. benthamiana* via agrobacterium. At 2 d post infiltration of Agrobacterium, the leaves pre-infiltrated with Agrobacterium were infected with Pto DC3000Q$^-$(AvrRpm2$_{Psa}$) at a high bacterial concentration (OD_{600}=1.0). There were no significant differences in RIN4 accumulation with Agrobacterium concentrations of OD_{600}=0.02 to 0.4. The *N. benthamiana* leaf areas infected with Pto DC3000Q$^-$(AvrRpm2$_{Psa}$) showed clear signs of infection at 15 h post infiltration (Figure 3A). At 1 d post infection of Pto DC3000Q$^-$(AvrRpm2$_{Psa}$), proteins were extracted from the infected leaves for Western blot analysis. The ADP-ribosylation of RIN4 was clearly detected from a Western blot prepared with the protein extracts without further fractionation or concentration (Figure 3B). In the transgenic Arabidopsis-Pto DC3000 system, expressing high concentration of proteins is difficult because host cells collapse as infections progress. In this Agrobacterium-DC3000Q$^-$ system in *N. benthamiana*, Agrobacterium-mediated transient expression prior to pathogen infection ensured high

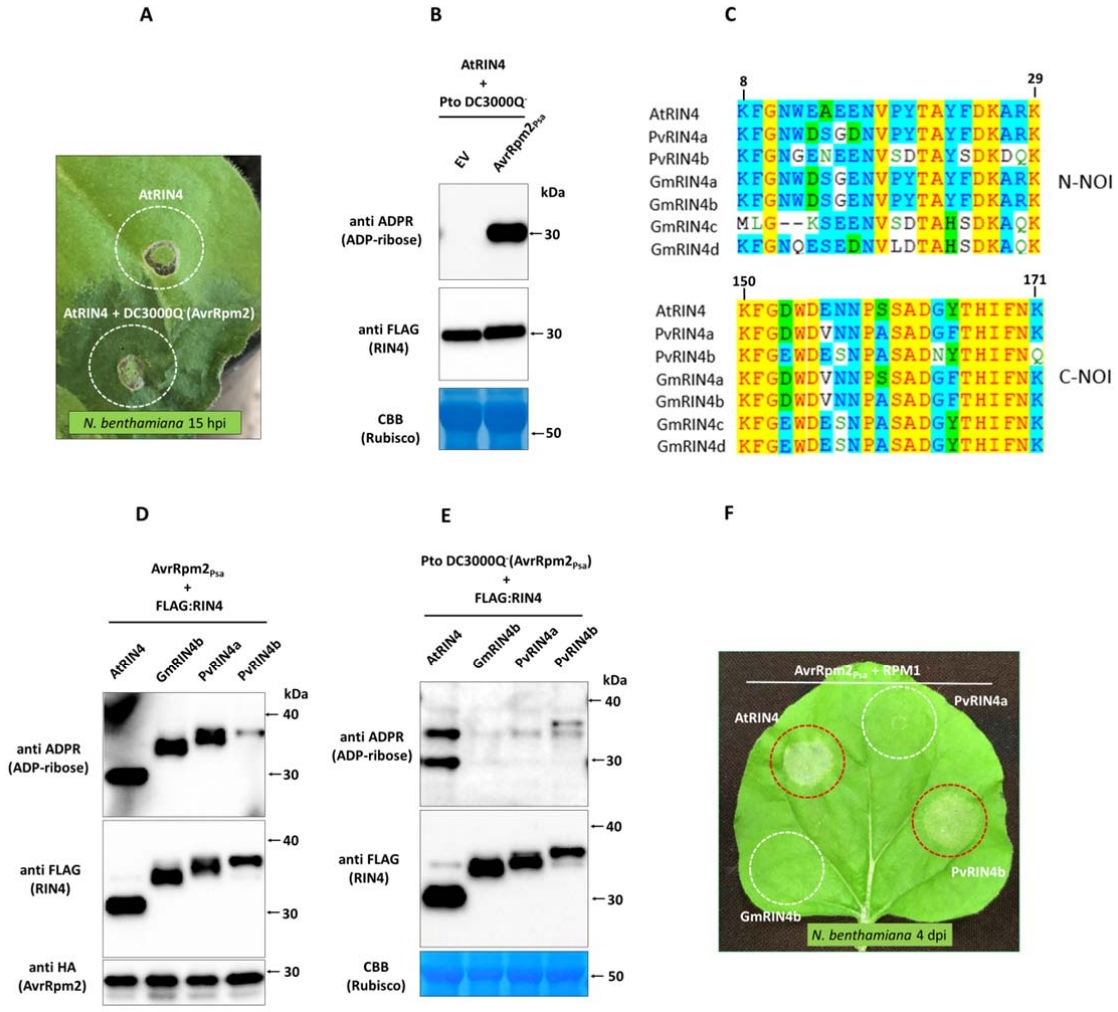

Figure 3. Secretion of bacterial effector via infection of Pto DC3000Q⁻ in *N. benthamiana*. **A**. An *N. benthamiana* leaf was infected with Pto DC3000Q⁻(AvrRpm2$_{Psa}$) at a high concentration (OD_{600}=1.0, or 5×10^8 cfu/mL) in the area pre-infiltrated with Agrobacterium 2 d earlier for transient expression of AtRIN4 (marked with a circle, bottom). Dark discolouration and leaf margin malformations indicate Pto infection. The control area infiltrated only with Agrobacterium is also marked (top). Image was taken at 15 h post infection. **B**. Western blot analysis demonstrated that AtRIN4 was ADP-ribosylated upon infection with Pto DC3000Q⁻(AvrRpm2$_{Psa}$). Proteins were extracted from *N. benthamiana* leaves expressing AtRIN4 via Agrobacterium after infection with Pto DC3000Q⁻(AvrRpm2$_{Psa}$). ADP-ribosylated proteins were detected using anti ADPR binding reagent. (EV: control Pto DC3000Q⁻ with an empty vector). **C**. Alignment of the two NOI sequences in RIN4 homologs of Arabidopsis (AtRIN4), snap bean (PvRIN4a and PvRIN4b) and soybean (GmRIN4a to GmRIN4d). **D**. Western blot analysis of RIN4 co-expressed with AvrRpm2$_{Psa}$ *in planta* via Agrobacterium. **E**. Western blot analysis of RIN4 homologs infected with Pto DC3000Q⁻(AvrRpm2$_{Psa}$). Proteins were extracted as in (**B**). **F**. The indicated RIN4 homologs were co-expressed with AvrRpm2$_{Psa}$ and RPM1 in different areas of an *N. benthamiana* leaf via Agrobacterium to assess the corresponding RPM1-mediated HR. Red circles denote HR and white circles denote no HR.

accumulation of RIN4 protein while through infection the expressed bacterial effector was efficiently secreted from the highly concentrated Pto DC3000Q⁻(AvrRpm2$_{Psa}$) into the host, facilitating the detection of the posttranslational modification.

Bacterial effectors expressed *in planta* via Agrobacterium may differ in activity to effectors translocated via T3SS

Among the four soybean RIN4 homologs, GmRIN4a and GmRIN4b were ADP-ribosylated when co-expressed with $AvrRpm1_{Pma}$ while GmRIN4c or GmRIN4d were not modified (Redditt et al., 2019). To compare $AvrRpm2_{Psa}$ expressed *in planta* via Agrobacterium with the bacterial effector secreted during an infection, we analysed the ADP-ribosylation in RIN4 homologs of Arabidopsis, soybean, and snap bean (AtRIN4, GmRIN4b, PvRIN4a, and PvRIN4b). PvRIN4a is more closely related to GmRIN4a and GmRIN4b, while PvRIN4b is more similar to GmRIN4c or GmRIN4d (Figure 3C). Proteins were extracted from *N. benthamiana* leaves co-expressing these RIN4 homologs and $AvrRpm2_{Psa}$ via Agrobacterium. Western blot analysis showed that all four RIN4 proteins were ADP-ribosylated (Figure 3D, anti ADPR). In particular, among the two snap bean RIN4 homologs, PvRIN4a was more strongly ADP-ribosylated compared with PvRIN4b. In the next, proteins were extracted from the leaves infected with Pto DC3000Q$^-$ ($AvrRpm2_{Psa}$) following transient expression of RIN4 homologs via Agrobacterium. Western blot analysis showed that only AtRIN4 and PvRIN4b were ADP-ribosylated and GmRIN4b and PvRIN4a were not modified (Figure 3E). Modifications in AtRIN4 or PvRIN4b were not significantly different between the two effector deliveries either by the Agrobacterium-mediated transient expression of $AvrRpm2_{Psa}$ or by the infection of Pto DC3000Q$^-$ ($AvrRpm2_{Psa}$).

Interestingly, when the RIN4 homologs were co-expressed with $AvrRpm2_{Psa}$ and RPM1 in *N. benthamiana* via Agrobacterium, only AtRIN4 and PvRIN4b triggered the RPM1-mediated HR (Figure 3F). In contrast, GmRIN4b or PvRIN4a resulted in no comparable HR even though they were also ADP-ribosylated by $AvrRpm2_{Psa}$ (Figure 3D). We reasoned that the ADP-ribosylation in GmRIN4b and PvRIN4a may have been caused by an unusual activity of the bacterial effector expressed *in planta* via Agrobacterium. Such modifications may be artefacts created in our experimental system and may not naturally occur during pathogen infection. We conclude that mass spectrometry analysis of a bacterial effector expressed *in planta* via Agrobacterium may not always lead to a *bona fide* identification of ADP-ribosylation catalysed by the T3SS-delivered bacterial effector during an infection.

Identification of the $AvrRpm2_{Psa}$ target site by mutational analysis

After carefully studying available mass spectra of AtRIN4 peptides, we hypothesised that the target sites are within the NOI domains, and performed mutational analysis by changing

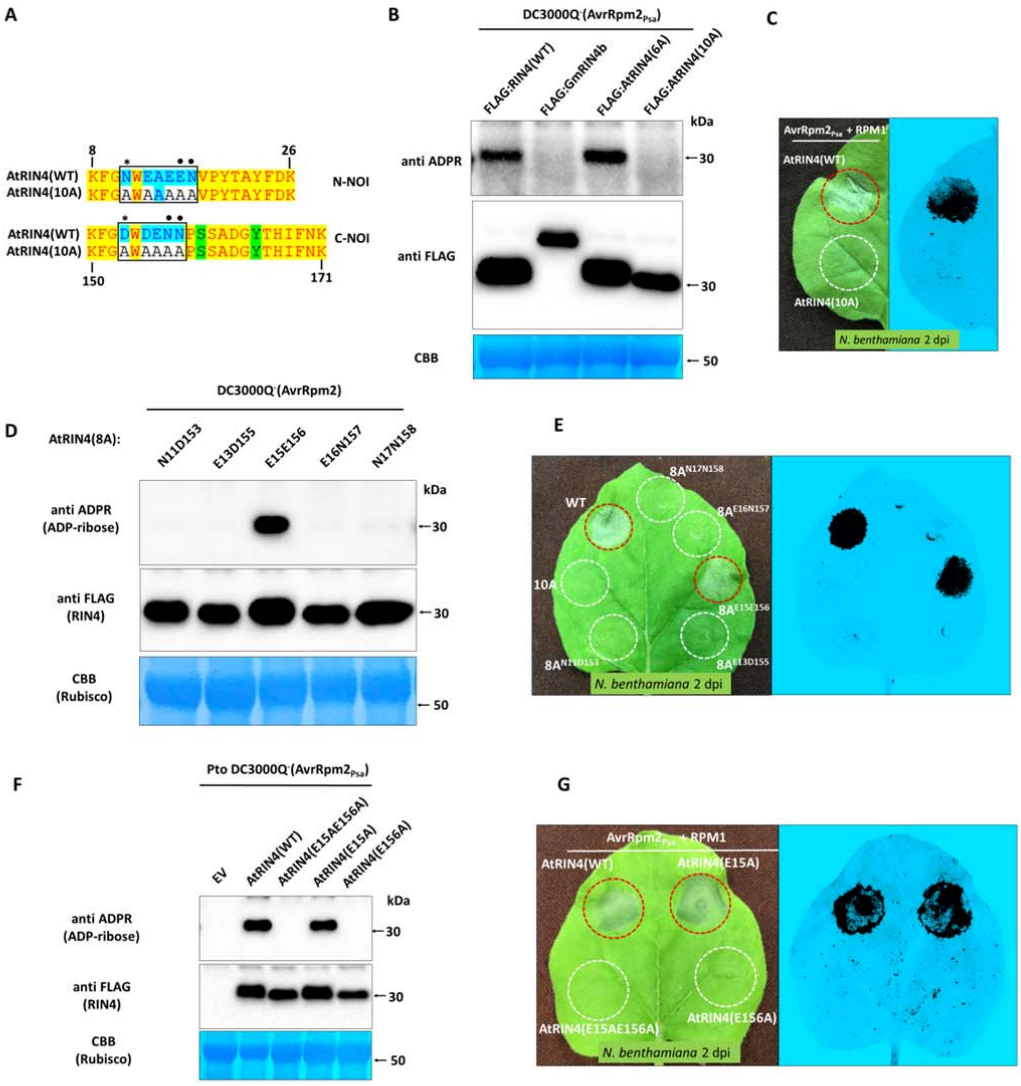

Figure 4. Identification of the target residue for AvrRpm2$_{Psa}$ by mutational analysis. **A**. Modifications generated in the two NOI sequences of AtRIN4 (top). The ten modifications in target amini acids N, D, and E (N11A, E13A, E15A, E16A, N17A, D153A, D155A, E156A, N157A, N158A) in AtRIN4^{10A} are boxed in black (□) and the six modifications in AtRIN4^{6A} (N11A, E16A, N17D, D153A, N157A, N158A) are marked with asterisk (* for the residues N11 and D153 identified as candidates previously) (Redditt et al., 2019) or closed circle (• in E16, N17, N157, and N158 identified as candidates by this study). AtRIN4^{10A} was co-expressed with AvrRpm2$_{Psa}$ and RPM1 in *N. benthamiana*, to assess the RPM1-mediated HR when (bottom). HR was assessed visually or by monitoring fluorescence with ChemiDoc™ at 2 d post Agrobacterium infiltration. **B**. Western blot analysis of RIN4 alleles (AtRIN4^{WT}, GmRIN4b^{WT}, AtRIN4^{6A} and AtRIN4^{10A}) from leaves infected with with Pto DC3000Q⁻(AvrRpm2$_{Psa}$) (left). Proteins were extracted 1 d post infection of Pto DC3000Q⁻(AvrRpm2) in *N. benthamiana* leaves pre-infiltrated with Agrobacterium 2 d earlier for transient expression of RIN4. To assess the RPM1-mediated HR, AtRIN4 proteins were co-expressed with AvrRpm2$_{Psa}$ and RPM1 in *N. benthamiana* (right). The fluorescence image captured in ChemiDoc™ at 2 d post Agrobacterium infiltration is shown. **C**. Western blot analysis of the five AtRIN4^{8A} variant proteins (AtRIN4$^{8A}{}_{E11D153}$, AtRIN4$^{8A}{}_{E13D155}$, AtRIN4$^{8A}{}_{E15E156}$, AtRIN4$^{8A}{}_{E16N157}$, and AtRIN4$^{8A}{}_{N17N158}$) from leaves infected with with Pto DC3000Q⁻(AvrRpm2$_{Psa}$). Proteins were extracted as in (**B**). **D**. The five AtRIN4^{8A} proteins were co-expressed with AvrRpm2$_{Psa}$ and RPM1 in *N. benthamiana* via Agrobacterium to assess the corresponding HR. Visual inspection (left) and fluorescence test using the ChemiDoc™ (right) are shown. **E**. Western blot analysis of AtRIN4 proteins (AtRIN4^{WT}, AtRIN4^{E15AE156A}, AtRIN4^{E15A}, and AtRIN4^{E156A}) from leaves infected with Pto DC3000Q⁻(AvrRpm2$_{Psa}$). Proteins were extracted as in (**B**). **F**. AtRIN4 proteins (AtRIN4^{WT}, AtRIN4^{E15AE156A}, AtRIN4^{E15A}, and AtRIN4^{E156A}) were co-expressed with AvrRpm2$_{Psa}$ and RPM1 in *N. benthamiana* to assess HR. The visual inspection (left) and the fluorescence test with the ChemiDoc™ (right) are shown. Red circles denote HR and white circles denote no HR.

candidate residues in the NOI domain sequences. Based on the results from previous mass spectrometry analyses, we tested AtRIN4^{6A}, in which the six residues (N11, E16, N17, D153, N157, and N158) collectively identified by earlier analyses as targets were replaced with alanine (A) to prevent modification on these sites (Figure 4A). Western blot analysis showed that AtRIN4^{6A} was still ADP-ribosylated by Pto DC3000Q⁻(AvrRpm2$_{Psa}$) (Figure 4B). We

further replaced four more residues to create AtRIN4^{10A}. The modified ten residues were the five amino acids (N11, E13, E15, E16, and N17) in the N-NOI domain and the corresponding five residues (D153, D155, E156, N157, and N158) in the C-NOI domain. Western blot analysis showed that AtRIN4^{10A} was no longer ADP-ribosylated by Pto DC3000Q^{-} (AvrRpm2$_{Psa}$) (Figure 4B). When AtRIN4^{10A} was co-expressed with RPM1 and AvrRpm2$_{Psa}$ in *N. benthamiana* via Agrobacterium, no HR was detected compared with AtRIN4^{WT}, suggesting RPM1 was not activated (Figure 4C, white circle). In the next step, we systematically reinstated two original residues at a time in AtRIN4^{10A} (one in the N-NOI domain and the corresponding other in the C-NOI domain) to create five different AtRIN4^{8A} alleles (AtRIN4$^{8A}_{N11D153,}$ AtRIN4$^{8A}_{E13D155,}$ AtRIN4$^{8A}_{E15E156,}$ AtRIN4$^{8A}_{N16N157}$, and AtRIN4$^{8A}_{N17N158}$). The five AtRIN4^{8A} proteins were transiently expressed in *N. benthamiana* via Agrobacterium and the leaves were infected with Pto DC3000Q^{-}(AvrRpm2$_{Psa}$). When proteins were extracted and Western blot analysis was performed, we found that ADP-ribosylation was restored in AtRIN4$^{8A}_{E15E156}$, while the other four AtRIN4^{8A} alleles were not modified by AvrRpm2$_{Psa}$ (Figure 4D). Accordingly, when the AtRIN4^{8A} proteins were co-expressed with AvrRpm2$_{Psa}$ and RPM1 in *N. benthamiana* via Agrobacterium, only AtRIN4$^{8A}_{E15E156}$ triggered the RPM1-mediated HR, matching the genotype with both the biochemical and physiological phenotypes (Figure 4E).

As AtRIN4$^{8A}_{E15E156}$ recovered ADP-ribosylation from AtRIN4^{10A}, the target residue(s) for the AvrRpm2$_{Psa}$ activity could be either E15, E156, or both residues. We created the double mutant allele AtRIN4^{E15AE156A}, which is the reciprocal modification of AtRIN4$^{8A}_{E15E156}$, as well as the two single mutant alleles AtRIN4^{E15A} and AtRIN4^{E156A}. They were transiently expressed in *N. benthamiana* via Agrobacterium and the leaves were infected with Pto DC3000Q^{-}(AvrRpm2$_{Psa}$) as above. Western blot analysis showed that AtRIN4^{E15AE156A} was not ADP-ribosylated as expected (Figure 4F). Out of the two individually modified proteins, AtRIN4^{E156A} was not ADP-ribosylated while AtRIN4^{E15A} was still modified, demonstrating that the glutamate (E156) in the C-NOI domain is the target site for AvrRpm2$_{Psa}$ during infection. When the AtRIN4 proteins were co-expressed with AvrRpm2$_{Psa}$ and RPM1 in *N. benthamiana* via Agrobacterium, the RPM1-mediated HR was lost with AtRIN4^{E156A} (Figure 4G, white circle) while the corresponding HR was still detected with AtRIN4^{E15A} (Figure 4G, red circles). Consistent with the earlier observation (Figure 1B), slower migration of ADP-ribosylated AtRIN4 during electrophoresis was detected in AtRIN4^{E15A} or AtRIN4^{WT}, but not in AtRIN4^{E156A} or AtRIN4^{E15AE156A} (Figure 4F).

Conserved glutamate residues in GmRIN4c and GmRIN4d are ADP-ribosylated by AvrRpm2$_{Psa}$

There are four soybean RIN4 homologs (Figure 5A). When co-expressed with AvrRpm1$_{Pma}$ in *N. benthamiana* via Agrobacterium, GmRIN4a and GmRIN4b were shown to be ADP-ribosylated while GmRIN4c or GmRIN4d were not modified (Redditt et al., 2019). In stark contrast, we found that GmRIN4c and GmRIN4d were ADP-ribosylated by Pto DC3000Q$^-$ (AvrRpm2$_{Psa}$) while GmRIN4a and GmRIN4b were not modified (Figure 5B). Accordingly, when the GmRIN4 homologs were co-expressed with AvrRpm2$_{Psa}$ and RPM1 in *N. benthamiana* via Agrobacterium, only GmRIN4c and GmRIN4d activated RPM1 (Figure 5C). The two homologs GmRIN4c and GmRIN4d have glutamate (E) residues at their respective positions corresponding to the E156 of AtRIN4. In contrast, GmRIN4a and GmRIN4b have valine (V) at these positions. Similarly, among the two RIN4 homologs of snap bean, PvRIN4b has the glutamate at the position corresponding to the E156 of AtRIN4 while PvRIN4a has valine at that position (Figure 3C). PvRIN4b was ADP-ribosylated with the infection of Pto DC3000Q$^-$(AvrRpm2$_{Psa}$) (Figure 3E) and also activated RPM1 when co-expressed with AvrRpm2$_{Psa}$ and RPM1 in *N. benthamiana* (Figure 3F). In contrast, PvRIN4a was not modified by Pto DC3000Q$^-$(AvrRpm2$_{Psa}$) and no corresponding HR was detected when co-expressed with AvrRpm2$_{Psa}$ and RPM1 in *N. benthamiana* via Agrobacterium. Therefore, the allelic variations in the critical residue within the C-NOI domains of soybean and snap bean RIN4 homologs were reflected in the differential ADP-ribosylation patterns by AvrRpm2$_{Psa}$, suggesting the conserved glutamate residues at the corresponding positions of the E156 of AtRIN4 are the likely target sites in these RIN4 homologs. Interestingly, the alternative residue valine is also found at the positions corresponding to E156 in other Arabidopsis NOI domain-containing proteins (Redditt et al., 2019).

To further study the functional significance of the glutamate residues in the two GmRIN4 homologs at the corresponding positions of E156 in AtRIN4 (E189 in GmRIN4c and E180 GmRIN4d, respectively), substitutions were made to create GmRIN4c^{E189A} and GmRIN4d^{E180A}. Proteins were extracted from *N. benthamiana* leaves expressing GmRIN4c^{E189A} or GmRIN4d^{E180A} via Agrobacterium after infection with Pto DC3000Q$^-$ (AvrRpm2$_{Psa}$). Western blot analysis showed that GmRIN4c^{E189A} was not ADP-ribosylated, demonstrating the replaced glutamate (E189) was the only target site for AvrRpm2$_{Psa}$ in

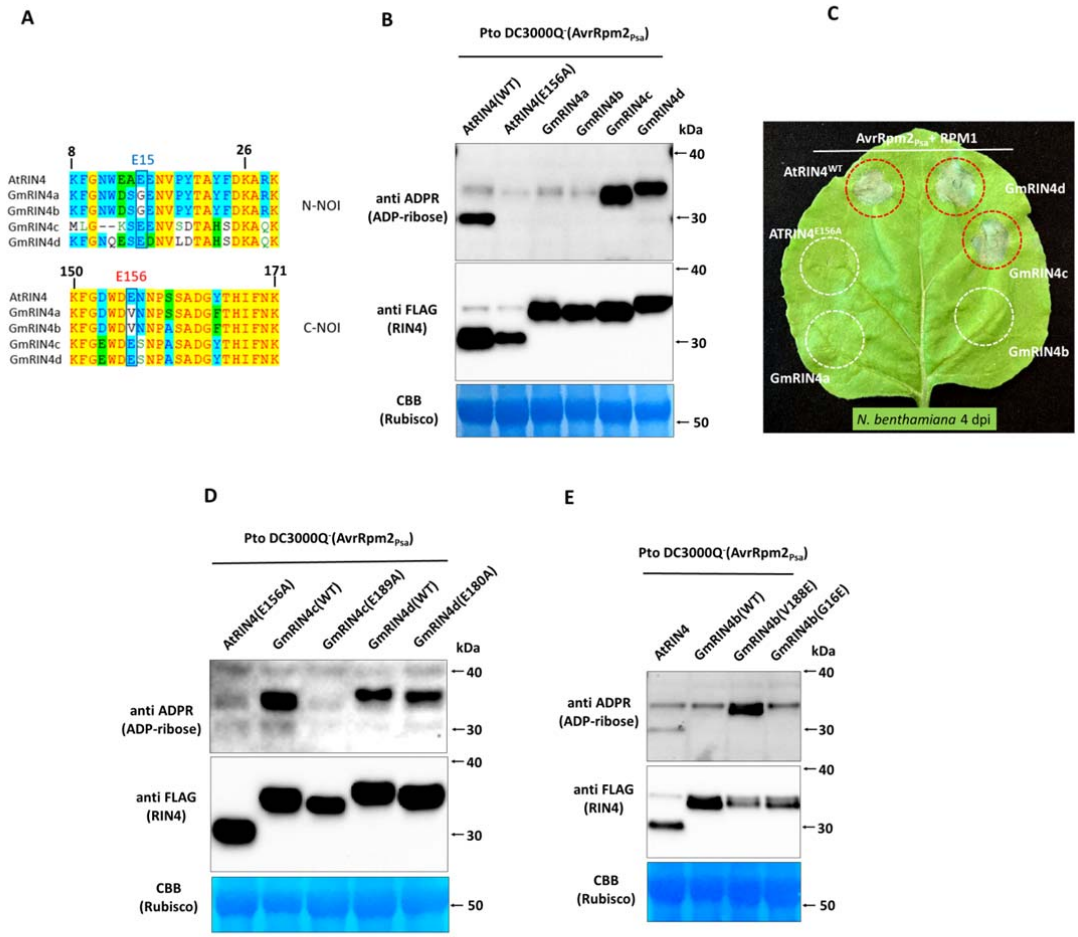

Figure 5. Western blot analysis of soybean RIN4 homologs from *N. benthamiana* leaves infected with Pto DC3000Q⁻(AvrRpm2$_{Psa}$). **A**. Sequence alignment of the nitrate-induced (NOI) sequences in RIN4 homologs of Arabidopsis (AtRIN4) and soybean (GmRIN4a, GmRIN4b, GmRIN4c, and GmRIN4d). E156 in AtRIN4 corresponds to E189 in GmRIN4c or E180 in GmRIN4d, respectively. GmRIN4a and GmRIN4b have a valine (V) at the corresponding positions. **B**. Western blot analysis of soybean RIN4 homologs after infection with Pto DC3000Q⁻(AvrRpm2$_{Psa}$). Proteins were extracted from *N. benthamiana* leaves 1 d post infiltration of Pto DC3000Q⁻(AvrRpm2$_{Psa}$) following Agrobacterium infiltration 2 d earlier for transient expression RIN4 homologs. **C**. Soybean RIN4 homologs were co-expressed with AvrRpm2$_{Psa}$ and RPM1 in *N. benthamiana* via Agrobacterium to assess the RPM1-mediated HR. The visual image was taken in 4 d post Agrobacterium infiltration. Red circles denote HR and white circles denote no HR. **D**. Western blot analysis of GmRIN4c^{E189A} and GmRIN4d^{E180A} from *N. benthamiana* leaves infected with Pto DC3000Q⁻(AvrRpm2$_{Psa}$). Proteins extraction and Western blot analysis were performed as in (**B**). **E**. Western blot analysis of GmRIN4b^{V188E} and GmRIN4b^{G16E} from *N. benthamiana* leaves infected with Pto DC3000Q⁻(AvrRpm2$_{Psa}$). Proteins extraction and Western blot analysis were performed as in (**B**).

GmRIN4c (Figure 5D). In contrast, GmRIN4d^{E180A} was still ADP-ribosylated even though the modification of the probable target site was blocked by the substitution (E180A). The ADP-ribosylated GmRIN4d^{E180A} consistently migrated faster than the ADP-ribosylated GmRIN4d^{WT} during electrophoresis (Figure 5D), suggesting potential differences in structure among RIN4 proteins modified at different sites. Unlike GmRIN4c, which has only one target site (E189), GmRIN4d appears to have other residue(s) that can be ADP-ribosylated when E180 is absent.

Apart from the position corresponding to E156 of AtRIN4 in the C-NOI domain, GmRIN4 homologs have another polymorphic site in the corresponding N-NOI domain at the position corresponding to E15 of AtRIN4 (Figure 5A). The soybean RIN4 homologs GmRIN4a and GmRIN4b have substitutions at these two positions when compared with AtRIN4 or the other two GmRIN4 homologs (Figure 5A). To further investigate the participation of these two glutamates in the ADP-ribosylation, we created GmRIN4b^{V188E} and GmRIN4b^{G16E} by instating glutamate residues at the positions corresponding to E156 or E15 of AtRIN4, respectively. Proteins were extracted from *N. benthamiana* leaves transiently expressing the modified GmRIN4b proteins after infection with Pto DC3000Q^{-}(AvrRpm2$_{Psa}$). Western blot analysis showed that GmRIN4b^{V188E} became efficiently ADP-ribosylated with a substituted glutamate at the site corresponding to E156 of AtRIN4, while the GmRIN4b^{G16E} with a substituted glutamate corresponding to E15 of AtRIN4 was not modified (Figure 5E). Therefore, the absence of the conserved glutamate residue corresponding to E156 of AtRIN4 is likely responsible for the lack of ADP-ribosylation in GmRIN4b by the bacterial effector AvrRpm2$_{Psa}$.

A conserved glutamate of MdRIN4-2 is ADP-ribosylated by AvrRpm2$_{Psa}$ and the N-NOI domain plays a role in HR

There are two RIN4 homologs in apple species. In contrast to GmRIN4 homologs, both MdRIN4 homologs have glutamates in the positions corresponding to the E156 of AtRIN4 (E186 in MdRIN4-2 and E184 in MdRIN4-1, Figure 6A). To see whether the E186 in MdRIN4-2 is also the target of AvrRpm2$_{Psa}$, we created MdRIN4-2^{E186A} to block the modification at this site. Proteins were extracted from *N. benthamiana* leaves transiently expressing MdRIN4-2^{E186A} via Agrobacterium after infection with Pto DC3000Q^{-} (AvrRpm2$_{Psa}$). Similar to AtRIN4^{E156A}, Western blot analysis showed that MdRIN4-2^{E186A} was not ADP-ribosylated (Figure 6B, left), suggesting that E186 is the likely target of AvrRpm2$_{Psa}$. When MdRIN4-2^{E186A} was co-expressed with AvrRpm2$_{Psa}$ and RPM1 in *N. benthamiana* via Agrobacterium, no significant HR was found compared with the wild type MdRIN4-2^{WT} (Figure 6B, right).

Because the C-NOI domains of the two apple RIN4 homologs are identical, two amino acids 15D and 16Q in the N-NOI domain of MdRIN4-1 are the only different residues in the two

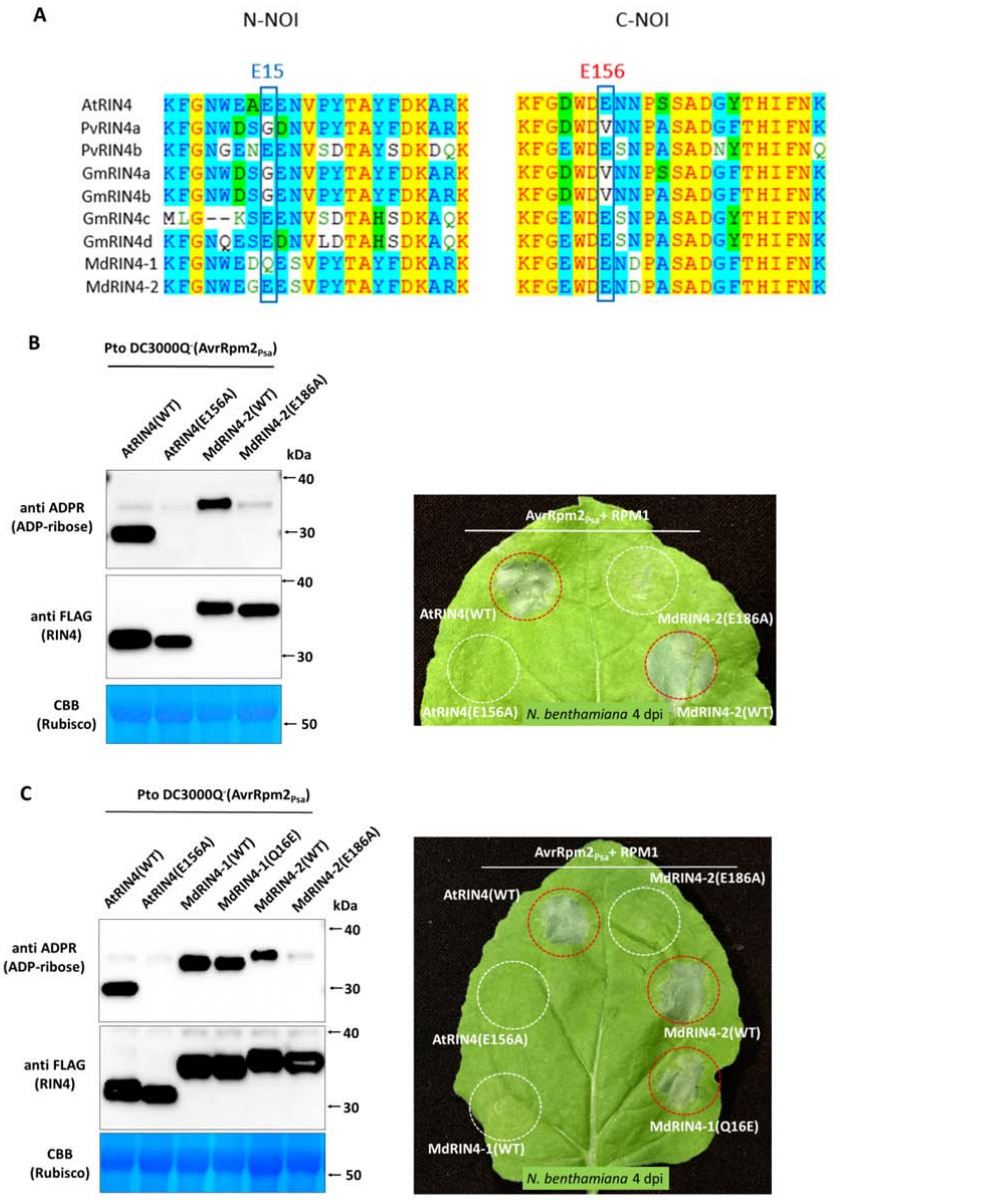

Figure 6. Western blot analysis and RPM1-mediated HR assay of apple RIN4 homologs. **A**. Sequence alignment of the NOI sequences in the RIN4 homologs of Arabidopsis (AtRIN4), snap bean (PvRIN4a and PvRIN4b), soybean (GmRIN4a to GmRIN4d), and apple (MdRIN4-1 and MdRIN4-2). Both apple RIN4 loci have glutamate residues at the positions (E186 in MdRIN4-2 and E184 in MdRIN4-1) corresponding to E156 of AtRIN4. MdRIN4-2 also has a glutamate (E16) at the position corresponding to E15 of AtRIN4, while MdRIN4-1 has an alternative residue glutamine (Q16). **B**. Western blot analysis of MdRIN4-2^{E186A} (left). Proteins were extracted 1 d post infection of Pto DC3000Q⁻(AvrRpm2$_{Psa}$) into *N. benthamiana* leaves that had been pre-infiltrated with Agrobacterium 2 d earlier for transient expression of RIN4 homologs. Apple RIN4 homologs were co-expressed with AvrRpm2$_{Psa}$ and RPM1 in *N. benthamiana* via Agrobacterium to assess the RPM1-mediated HR (right). **C**. Western blot analysis of MdRIN4-1^{Q16E} with other RIN4 homologs (left). Protein extractions and Western blot analysis were performed as in (**B**). MdRIN4-1^{Q16E} and other RIN4 homologs were co-expressed with AvrRpm2$_{Psa}$ and RPM1 via Agrobacterium in different areas of an *N. benthamiana* leaf to assess the RPM1-mediated HR.

NOI sequenences when compared with MdRIN4-2. In particular, MdRIN4-2 has a glutamate (E16) in the N-NOI domain at the position corresponding to E15 in AtRIN4, while MdRIN4-1 has glutamine (Q16) at the corresponding position (Figure 6A). Both homologs were ADP-ribosylated by Pto DC3000Q⁻(AvrRpm2$_{Psa}$) as expected (Figure 6C, left). However, when co-expressed with AvrRpm2$_{Psa}$ and AtRIN4 in *N. benthamiana* via Agrobacterium, MdRIN4-1

435 did not trigger the RPM1-mediated HR, suggesting that the ADP-ribosylation of MdRIN4-1
436 by AvrRpm2$_{Psa}$ may not be recognised by RPM1 (Figure 6C, right). We created MdRIN4-
437 1^{Q16E} to substitute a glutamate in place of Q16 and tested whether the glutamate at this
438 position would affect the activity. Proteins were extracted from *N. benthamiana* leaves after
439 infection with Pto DC3000Q^{-}(AvrRpm2$_{Psa}$) following transient expression of MdRIN4-1^{Q16E}
440 via Agrobacterium. Western blot analysis showed no significant changes in ADP-ribosylation
441 or protein accumulation of MdRIN4-1^{Q16E} compared with the wild type MdRIN4-1^{WT} (Figure
442 6C, left). However, when MdRIN4-1^{Q16E} was co-expressed with RPM1 and AvrRpm2$_{Psa}$ in *N.*
443 *benthamiana* via Agrobacterium, an RPM1-mediated HR was observed (Figure 5C, right).
444 The substitution of the glutamate in MdRIN4-1^{Q16E} at the position corresponding to E15 of
445 AtRIN4 resulted in an activation of RPM1, comparable with that of MdRIN4-2. Therefore,
446 even though E16 in MdRIN4-2 (and also in MdRIN4-1^{Q16E}) is not modified by AvrRpm2$_{Psa}$,
447 the glutamate residue appears to be also important in activating RPM1. It is interesting to note
448 that apple species also have MdRIN4-1, which is ADP-ribosylated but does not activate
449 RPM1, in addition to the functional MdRIN4-2, which is ADP-ribosylated and activates
450 RPM1. It is possible that the ADP-ribosylation in MdRIN4-1 may be specifically recognised
451 by an apple resistance protein. Alternatively, the host may express a less sensitive RIN4 as
452 well as the fully functional RIN4 to reduce the cost of defence by attenuating unnecessary
453 responses.

454

455 **ADP-ribosylation of RIN4 may not be directly linked to phosphorylation**

456 Another effector AvrB from *Pseudomonas syringae* pv. *glycinea* is known to trigger RPM1
457 activation by inducing phosphorylation at T166 of AtRIN4 (Chung et al., 2011; Lee et al.,
458 2015a). The enzymatic activity of AvrB is not known but the phosphorylation of RIN4 is
459 thought to be mediated by plant kinases such as RIPK (Liu et al., 2011). A previous *in vitro*
460 experiment combined with mass spectrometry analysis suggested that RIPK may have three
461 target residues (T21, S160, and T166) in AtRIN4 (Liu et al., 2011). In particular, the
462 phosphorylation of T166 was proposed as a key physiological switch for defence (Chung et
463 al., 2014). Two other bacterial effectors AvrRpm1$_{Pma}$ and AvrRpm2$_{Psa}$ also trigger the
464 activation of RPM1. In particular, AvrRpm2$_{Psa}$ activates RPM1 by directly ADP-ribosylating
465 E156 of AtRIN4 (Figure 4F and 4G). Therefore, we investigated the impact of the ADP-

ribosylation of E156 on the phosphorylation at T166, and *vice versa*, in the RPM1-mediated HR in *N. benthamiana*.

Proteins were extracted from *N. benthamiana* leaves transiently co-expressing RIN4 homologs of Arabidopsis and soybean with AvrB via Agrobacterium. Western blot analysis showed that the RIN4 proteins were not ADP-ribosylated, suggesting that AvrB does not function as an ADP-ribosyl transferase to modify RIN4 (Figure 7A). When the triple mutant AtRIN4^{T21AS160AT166A}, in which the potential phosphorylation sites were blocked, was co-expressed with AvrB and RPM1 in *N. benthamiana* via Agrobacterium, there was a significant reduction in the HR compared with AtRIN4^{WT} (Figure 7B, white circle in the right half of the leaf), showing that the AvrB-triggered RPM1 activation depends on these replaced residues as previously reported (Chung et al., 2011). In contrast, when the ADP-ribosylation-deficient allele AtRIN4^{E156A} was co-expressed with AvrB and RPM1, no significant difference was found in the HR compared with the wild type AtRIN4^{WT} (Figure 7B, right half of the leaf). The absence of the ADP-ribosylation site (E156) in AtRIN4^{E156A} had no impact on the AvrB-triggered activation of RPM1. Therefore the AvrB-triggered, phosphorylation-dependent, activation of RPM1 appears not to depend on the ADP-ribosylation of E156 in AtRIN4.

In turn, when the phosphorylation-deficient mutant AtRIN4^{T21AS160AT166A} was co-expressed with AvrRpm2$_{Psa}$ and RPM1 in *N. benthamiana* via Agrobacterium, again there was no significant difference in the RPM1-mediated HR compared with the wild type AtRIN4^{WT}, while AtRIN4^{E156A} resulted in no host response (Figure 7B, left half of the leaf). Therefore, the AvrRpm2$_{Psa}$-triggered, ADP-ribosylation-dependent, activation of RPM1 appears not to rely on the phosphorylation of those modified sites, including T166. We also tested AtRIN4 alleles with substitutions at the phosphorylation sites in different combinations (AtRIN4^{T21A}, AtRIN4^{T166A}, AtRIN4^{T21AT166A}, and AtRIN4^{T21AS160AT166A}) with infection of Pto DC3000Q^{-} (AvrRpm2$_{Psa}$) instead of Agrobacterium-mediated transient expression. Western blot analysis showed no significant differences in ADP-ribosylation between AtRIN4^{WT}, AtRIN4^{T21A}, AtRIN4^{T166A}, AtRIN4^{T21AT166A}, or AtRIN4^{T21AS160AT166A}, while AtRIN4^{E156A} showed no ADP-ribosylation (Figure 7C, left). Accordingly, when the RIN4 alleles were co-expressed with AvrRpm2$_{Psa}$ and RPM1 in *N. benthamiana* via Agrobacterium, all resulted in comparable host responses except AtRIN4^{E156A} (Figure 7C, right).

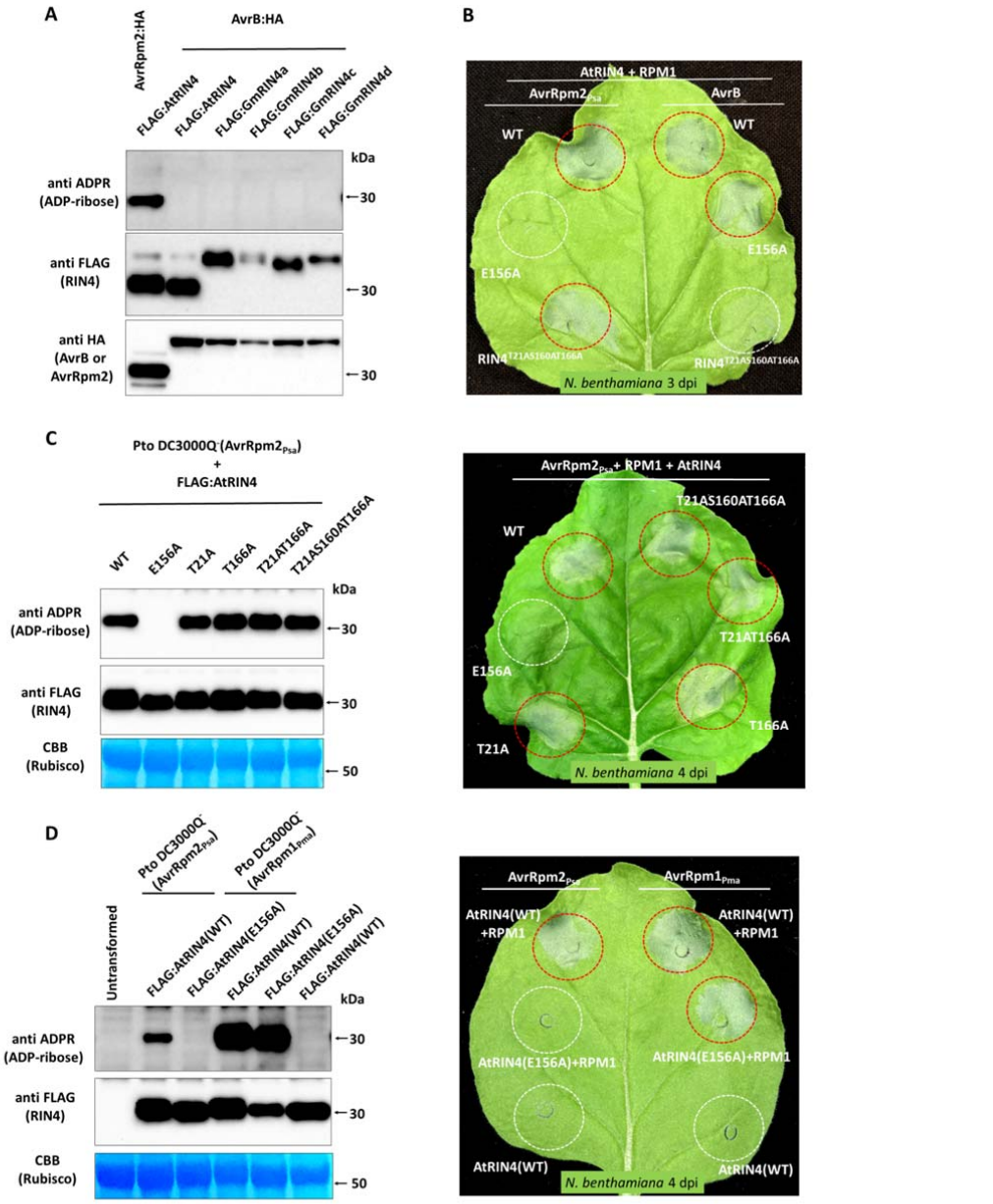

Figure 7. Activities of the type three effectors (T3Es) triggering RPM1 activation. **A**. Western blot analysis of RIN4 homologs of Arabidopsis (AtRIN4) and soybean (GmRIIN4a to GmRIN4d) co-expressed in *N. benthamiana* via Agrobacterium. Proteins were extracted from *N. benthamiana* leaves co-expressing AvrB with RIN4 via Agrobacterium at 2 d post infiltration. **B**. Different AtRIN4 alleles (AtRIN4^{WT}, AtRIN4^{E156A} or AtRIN4^{T21AS1690AT166A}) and RPM1 were co-expressed with either AvrRpm2$_{Psa}$ (left half) or AvrB (right half) on an *N. benthamiana* leaf via Agrobacterium to assess the corresponding RPM1-mediated HR. **C**. Western blot analysis of different AtRIN4 alleles (AtRIN4^{WT}, AtRIN4^{E156A}, AtRIN4^{T21A}, AtRIN4^{T166A}, AtRIN4^{T21AT166A}, and AtRIN4^{T21AS1690AT166A}) from *N. benthamiana* leaves infected with Pto DC3000Q$^-$(AvrRpm2$_{Psa}$) (left). Proteins were extracted 1 d post infection of Pto DC3000Q$^-$(AvrRpm2$_{Psa}$) into *N. benthamiana* leaves pre-infiltrated with Agrobacterium 2 d earlier for transient expression of the RIN4 alleles. The AtRIN4 alleles were co-expressed with AvrRpm2$_{Psa}$ and RPM1 on different areas of an *N. benthamiana* leaf via Agrobacterium (right). **D**. Western blot analysis of AtRIN4^{E156A} from *N. benthamiana* leaves infected with either Pto DC3000Q$^-$(AvrRpm2$_{Psa}$) or by Pto DC3000Q$^-$(AvrRpm1$_{Pma}$) (left). AtRIN4^{E156A} and RPM1 were co-expressed with either AvrRpm2$_{Psa}$ or AvrRpm1$_{Pma}$ on different areas of an *N. benthamiana* leaf to assess the RPM1-mediated HR (right). Red circles denote HR and white circles denote no HR.

Even though the two posttranslational modifications, ADP-ribosylation and phosphorylation, of RIN4 are closely linked to the activation of RPM1, they may not be equivalent physiologically as well as biochemically. Because a secreted bacterial effector directly modifies the host protein, ADP-ribosylation of RIN4 by AvrRpm2$_{Psa}$ may be one of the

pathogen's virulence activities. In contrast, the phosphorylation of RIN4 by host kinases is more likely to be a part of defence mechanism responding to a bacterial protein. RPM1 may be independently activated either by the direct ADP-ribosylation of E156 or by the phosphorylation of T166 so long as either modification is recognised by the resistance protein, which is physically associated in the RIN4 multi-protein complex. To our current knowledge, there is no known biochemical activity of AvrB apart from a strong affinity to RIN4. Therefore, AvrB may induce phosphorylation of RIN4 by changing the interactions between proteins, including RIPK and RPM1 in Arabidopsis, in the RIN4 complex. In contrast, AvrRpm2$_{Psa}$ directly modifies RIN4 to generate a distinct structural change, which may affect other physically associated proteins in the multi-protein complex including RPM1 in Arabidopsis.

Apart from the RPM1 activation, we have little knowledge about the physiological significance of the structural change introduced in the RIN4 complex by AvrRpm2$_{Psa}$. It would be interesting to see whether the ADP-ribosylation of RIN4 would affect the activities of other proteins in the RIN4 complex. Interestingly, AvrRpm2$_{Psa}$ also physically associates with RIN4 (Figure 2A), therefore it is possible that the bacterial protein has the ability to change protein-protein interactions in the RIN4 multi-protein complex even without modifying RIN4.

AvrRpm2$_{Psa}$ and AvrRpm1$_{Pma}$ have distinct properties

The bacterial effector AvrRpm1$_{Pma}$ also functions as an ADP-ribosyl transferase to modify RIN4, leading to the activation of RPM1 (Redditt et al., 2019). To compare the activities of AvrRpm1$_{Pma}$ and AvrRpm2$_{Psa}$, we tested AvrRpm1$_{Pma}$ in combination with AtRIN4^{E156A}, which cannot be ADP-ribosylated by AvrRpm2$_{Psa}$. When proteins were extracted from *N. benthamiana* leaves infected with Pto DC3000Q^{-}(AvrRpm1$_{Pma}$) following transient expression of AtRIN4^{E156A} via Agrobacterium, Western blot analysis showed that AtRIN4^{E156A} was still ADP-ribosylated, demonstrating that another residue was modified by AvrRpm1$_{Pma}$ (Figure 7D, left). When AvrRpm1$_{Pma}$ was co-expressed with AtRIN4^{E156A} and RPM1 in *N. benthamiana* via Agrobacterium, the corresponding RPM1-mediated HR was detected, while no comparable HR was found with AvrRpm2$_{Psa}$ (Figure 7D, right). AvrRpm1$_{Pma}$ and AvrRpm2$_{Psa}$ also showed completely different activities when tested with

GmRIN4 homologs (Figure 5B and Figure S4). Therefore, the activities of these two effectors are not biochemically identical. AvrRpm1$_{Pma}$ and AvrRpm2$_{Psa}$ are the only two ADP-ribosyl transferases (ARTs) from bacterial plant pathogens so far characterised. However, sequence comparisons suggest that ARTs may be widely-distributed among phytopathogens colonising various plant hosts. RPM1 is an Arabidopsis protein and no close homologs are found in most other non-Brassicaceae plant species. Considering most plant species express RIN4 homologs and bacterial ARTs are found in non-Arabidopsis pathogens such as Psa (McCann et al., 2013; Fujikawa and Sawada, 2016; McCann et al., 2017), this posttranslational modification is likely to have other functional significance apart from the RPM1-mediated host response.

AvrRpm2$_{Psa}$ alleles have differential characteristics in activity and affinity

Based on genetic diversity and toxin production, Psa has been categorized into biovars (bv) (Fujikawa and Sawada, 2016, 2019). Recently bv4 has been transferred to another pathovar, *Pseudomonas syringae* pv. *actinidifoliorum* (Abelleira et al., 2015) and Psa is composed of five bvs currently. Apart from the recently added bv6, all other bvs have AvrRpm2$_{Psa}$ loci. The AvrRpm2$_{Psa}$ alleles in bv1 and bv3 have frameshift mutations, leading to premature termination of the corresponding proteins (Figure 8A). In addition to the frameshift mutations, the AvrRpm2$_{Psa}$ alleles in bv1 and bv3 also have two other independent substitutions when compared with the functional allele in bv5 (AvrRpm2$_{Psa}^{bv5}$ or simply AvrRpm2$_{Psa}$). We corrected the frameshifts in the bv1 and bv3 alleles by removing extra nucleotides to express the corresponding full length AvrRpm2$_{Psa}$ proteins. Western blot analysis showed that the edited proteins are expressed in full length (AvrRpm2$_{Psa}^{bv1(in\text{-}frame)}$ and AvrRpm2$_{Psa}^{bv3(in\text{-}frame)}$) in *N. benthamiana* (Figure 8B, anti HA in Input panel). However, when the edited proteins were co-expressed with AtRIN4, neither AvrRpm2$_{Psa}^{bv1(in\text{-}frame)}$ nor AvrRpm2$_{Psa}^{bv3(in\text{-}frame)}$ modified AtRIN4 (Figure 8B, anti ADPR in Input panel). The frameshift mutations in the bv1 and bv3 alleles are likely to be chronologically the last mutations in these alleles because non-functional genes would only accumulate random mutations. Therefore, the AvrRpm2$_{Psa}$ effectors in bv1 and bv3 appear to have lost their activity to modify RIN4 even before the frameshift mutations were selected.

Co-IP analysis with AtRIN4 showed that AvrRpm2$_{Psa}$ proteins from different bvs physically associate with AtRIN4 with differential affinities (Figure 8B, Co-IP panel). In particular, the

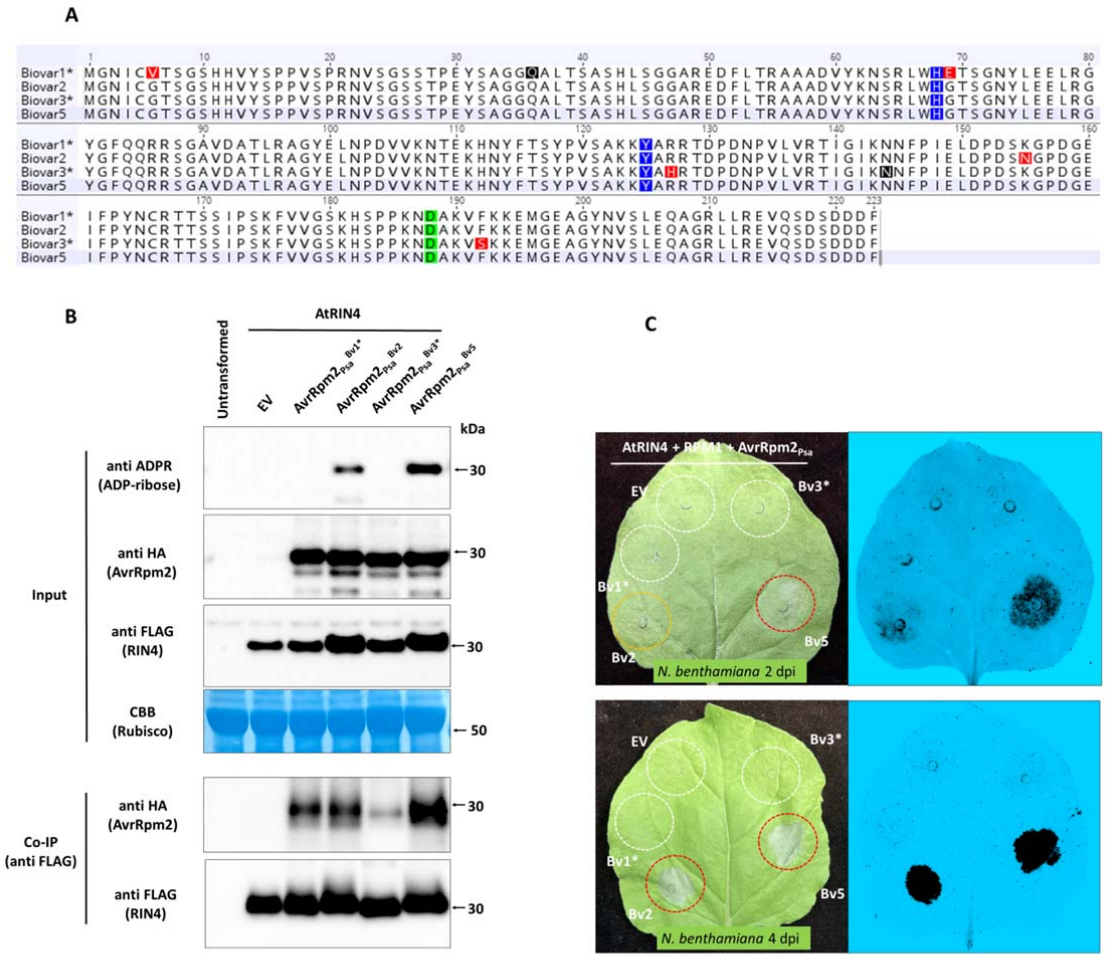

Figure 8. Activity and physical association of AvrRpm2$_{Psa}$ alleles. **A**. Sequence alignment of AvrRpm2$_{Psa}$ alleles from different Psa biovars. The biovar1 and biovar3 alleles were edited to express corresponding full-length proteins by removing extra nucleotides. The corrected sites are marked in black. The two residues H68 and Y125 are marked in blue and D188 is in green. All other substitutions are marked in red. **B**. Western blot analysis of AtRIN4 co-expressed with different AvrRpm2$_{Psa}$ alleles (input panel). Proteins were extracted 2 d after co-infiltration of AtRIN4 and AvrRpm2$_{Psa}$ in *N. benthamiana* via Agrobacterium. Co-IP of AtRIN4 with different AvrRpm2$_{Psa}$ proteins (Co-IP panel). Proteins were immunoprecipitated using anti FLAG magnetic beads to isolate AtRIN4. The precipitated proteins were probed using corresponding antibodies. **C**. AvrRpm2$_{Psa}$ alleles from different Psa biovars were co-expressed with AtRIN4 and RPM1 via Agrobacterium on different areas of an *N. benthamiana* leaf to assess the RPM1-mediated HR. Red circles denote HR, white circles denote no HR, and orange circle denotes reduced HR. Visual inspection (left) and fluorescence detection monitored in the ChemiDoc™ system (right) were shown.

physical association of AtRIN4 with AvrRpm2$_{Psa}^{bv3(in\text{-}frame)}$ was significantly lower when compared with AvrRpm2$_{Psa}^{bv5}$. The two other substitutions in AvrRpm2$_{Psa}^{bv3(in\text{-}frame)}$ are R127H and F192S, close to residues Y125 and D188, respectively, which correspond to the two residues in the conserved H-Y-D motif in AvrRpm1$_{Pma}$ (Cherkis et al., 2012). Earlier we found that AvrRpm2$_{Psa}^{Y125A}$ lost its catalytic activity while AvrRpm2$_{Psa}^{D188A}$ lost the ability for physical association with RIN4 (Figure 2C). Therefore the current AvrRpm2$_{Psa}^{bv3}$ allele may have undergone multiple selections to change its ability to affect the RIN4 protein complex (either by ADP-ribosylation of RIN4 or by changing physical association with RIN4). Similarly, the bv1 allele (AvrRpm2$_{Psa}^{bv1}$) has two other substitutions in addition to the

572 frameshift mutation when compared with the functional AvrRpm2$_{Psa}^{bv5}$. One substitution is
573 G69E, which is next to H68, another residue in the H-Y-D motif. The other substitution in the
574 AvrRpm2$_{Psa}^{bv1}$ is G6V. Glycine residues located near N-termini of bacterial effectors are
575 often involved in localisation of the bacterial proteins to membranes and this substitution may
576 have changed the localisation of the bacterial effector in the host.

577 The main activities of AvrRpm2$_{Psa}^{bv1(in\text{-}frame)}$ or AvrRpm2$_{Psa}^{bv3(in\text{-}frame)}$ may not have been the
578 ADP-ribosylation of RIN4. Otherwise, additional frameshift mutations would not have been
579 selected for these loci, which presumably had lost the activities already. AvrRpm2$_{Psa}^{bv1(in\text{-}frame)}$
580 may be able to affect the structure of the RIN4 multi-protein complex with a reduced affinity
581 to RIN4 (Figure 8B, CoIP) even though it does not modify RIN4. In contrast,
582 AvrRpm2$_{Psa}^{bv3(in\text{-}frame)}$ binds to RIN4 significantly weakly, suggesting that this bacterial
583 protein may affect the RIN4 complex neither by direct modification of RIN4 nor by the
584 physical association with RIN4. It is also possible that AvrRpm2$_{Psa}^{bv3(in\text{-}frame)}$ may have
585 differential affinities for different RIN4 homologs, specifically affecting protein-protein
586 interactions in different RIN4 complexes without modifying RIN4. Alternatively, considering
587 another bacterial ADP-ribosyl transferase AvrRpm1$_{Pma}$ specifically modified at least ten
588 other Arabidopsis proteins containing NOI domains (Redditt et al., 2019), AvrRpm2$_{Psa}^{bv1(in\text{-}frame)}$
589 and AvrRpm2$_{Psa}^{bv3(in\text{-}frame)}$ may have performed other virulence functions, which were
590 phased out by multiple selections, by targeting other proteins.

591 The allelic variations in the AvrRpm2$_{Psa}$ loci among bv1, bv3, and bv5 demonstrate the
592 importance of the residues around the H-Y-D motif. In contrast, the allele from bv2
593 (AvrRpm2$_{Psa}^{bv2}$) is catalytically functional with a single substitution (K155N) when
594 compared with AvrRpm2$_{Psa}^{bv5}$ (Figure 8B and Figure 8C). When co-expressed with RPM1
595 and AtRIN4 in *N. benthamiana* via Agrobacterium, this allele triggered significantly weaker
596 (or slower) HR compared with AvrRpm2$_{Psa}^{bv5}$ (Figure 8C, orange circle in 2 dpi). Co-IP
597 analysis suggests that AvrRpm2$_{Psa}^{bv2}$ physically associates with RIN4 with a reduced affinity
598 compared with AvrRpm2$_{Psa}^{bv5}$. The replaced residue N155 is distantly located from the H-Y-
599 D motif. It appears that the N155K substitution did not result in the complete loss of catalytic
600 activity (Figure 8B, anti ADPR in Input) nor the ability to physically associate with RIN4
601 (Figure 8B, anti HA in Co-IP).

602 Lastly, the allelic variations in the AvrRpm2$_{Psa}$ loci among modern day Psa biovars suggests
603 that there have been substantial interactions between the pathogen and the host relating to

604 these loci, raising a strong possibility that the Psa effector AvrRpm2$_{Psa}$ is recognised in its
605 natural host kiwifruit.

606

607

METHODS

Plant material, DNA constructs, bacterial strains, and growth conditions

For Agrobacterium-mediated transient expression, open reading frames of AvrRpm2$_{Psa}$ alleles were PCR amplified from respective Psa strains using a primer pair including a reverse primer that contained a HA tag sequence (AR2atgf1 and AR2HAtgar1) listed below. Amplified fragments were cloned in a binary vector (pART27, pHEX, or pGWB) under the 35S promoter to transform the Agrobacterium strain GV3101. The AvrRpm2$_{Psa}$ allele cloned from Psa biovar 5 was used in all experiments unless specified. For Pto infection, a 1.6 Kb genomic AvrRpm2$_{Psa}$ sequence including the *hrpL* box and the linked *ShcF* locus was PCR-amplified from Psa (biovar 5) using a primer pair gAR2psaf1 and gAR2psar1 (listed below). The amplified fragment was cloned in the broad-range vector pBBR1MCS5 to transform Pto DC3000Q$^-$, which has was created by deleting the hopQ1 locus (Yoon and Rikkerink, 2020). Constructs containing the AvrRpm1$_{Pma}$ locus were generated from synthesised DNA (a 947 bp EcoRI-EcoRV fragment from *Pseudomonas syringae* pv. *maculicola* plasmid pFKN, based on the Genbank sequence AF359557) with the set of primers (gAR1f1, AR1atgf1, AR1taar1, and AR1HAtgar1) listed below. Other related alleles required for transient expression or infection analyses were either created using the QuickChange Site-directed Mutagenesis Kit (Agilent Technologies, Santa Clara, CA) or synthesised by Twist Bioscience (South San Francisco, CA). *Nicotiana benthamiana* plants were grown at 22°C in long-day conditions (16 h light and 8 h dark) for both Agrobacterium-mediated transient expression and Pto DC3000Q$^-$ infection assays. Agrobacterium was freshly grown in LB with appropriate antibiotics at 28°C on a shaker. Cells were concentrated by centrifugation at 4000 g for 10 min and resuspended in infiltration buffer (10 mM $MgCl_2$, 100 µM acetosyringone). The cells were diluted to the appropriate concentrations (OD_{600} = 0.01- 0.08) and infiltrated into leaf tissues of 4- to 5-week-old plants using a needleless syringe. For the infection experiment, Pto DC3000Q$^-$ was re-streaked on a solid King's B media and re-grown at 28°C for 1 d. The freshly grown Pto DC3000Q$^-$ cells were suspended in 10 mM $MgCl_2$ for injection. To detect the cell death response in *N. benthamiana*, the Agrobacterium-infiltrated leaves were visually inspected at 2-5 days post infiltration and/or the fluorescence of the infiltrated leaves were monitored at 1-2 d post infiltration under the Pro-Q Emerald 488 in the ChemiDoc™ Gel Imaging System (Bio-Rad, Hercules, CA, USA) as described previously (Yoon and Rikkerink 2020).

640

641 **Agrobacterium-mediated transient expression and pathogen infection in *N.***
642 ***benthamiana***

643 For all plant transformations, the Agrobacterium strain GV3101 was transformed by
644 electroporation with a binary vector (pART27, pHEX2, or pGWB) containing a specified
645 construct under the 35S promoter. For transient expression, 4-5 weeks old *N. benthamiana*
646 leaves were syringe-infiltrated with Agrobacterium suspension (OD_{600}=0.01 to 0.08) carrying
647 the expression construct. A new sequential assay combined the Agrobacterium-mediated
648 transient expression of a host protein with pathogen infection to deliver bacterial effectors
649 with the T3SS. In such an assay *N. benthamiana* leaves were first infiltrated with
650 Agrobacterium, carrying the specified plant geneexpression construct, which was freshly
651 grown in LB media and adjusted to OD_{600}=0.04. Two d post Agrobacterium infiltration, the
652 pre-infiltrated *N. benthamiana* leaves were infected using a needleless syringe with a Pto
653 strain DC3000 without hopQ1 (Pto DC3000Q^-) (Wei et al., 2007) (Yoon and Rikkerink,
654 2020), carrying the bacterial effector. The Pto suspension was derived from freshly grown
655 Pto in King's B media and adjusted to OD_{600}=1.0. Leaf discs were collected at 15-24 h post
656 Pto infection for protein extraction before leaves collapsed due to the progression of the
657 infection.

658

659 **Western blot analysis and co-immunoprecipitation**

660 Western blot analysis and co-immunoprecipitation (Co-IP) were performed as previously
661 described with some modifications (Yoon and Rikkerink, 2020). For immunoblot analysis,
662 two leaf discs (8 mm diameter) were collected from infiltrated areas of the leaves and placed
663 in microfuge tubes containing cold 250 µL of extraction buffer (2% SDS, 10% glycerol in
664 PBS). Tissues were homogenised on ice using a micro-pestle and incubated at 90°C for 8
665 min and centrifuged at 16000 g for 2 min to collect the supernatant. Aliquots were run on a
666 4–12% SDS-PAGE gradient gel and electrophoresed proteins were transferred to a PDVF
667 membrane (Immobilon-P, Millipore, Burlington, MA, USA). To facilitate detection, an in
668 frame C-terminal HA tag was added onto effector sequences (avrRpm2$_{Psa}$, avrRpm1$_{Pma}$ or
669 AvrB) and an in frame N-terminal FLAG tag was added onto RIN4 homolog plant sequences.
670 Primary antibodies were used at a 1:5000 dilution and an anti-mouse secondary antibody

(A9044, Sigma-Adrich) was used at a 1:10 000 dilution. For Co-IP analyses, Agrobacterium-infiltrated *N. benthamiana* tissues were collected 2 d post infiltration. A 0.5 g sample of the collected tissues were ground under liquid nitrogen and suspended in 1 ml of co-IP extraction buffer (1× PBS, 1% n-dodecyl-β-d-maltoside (Invitrogen, Carlsbad, CA), protease inhibitor cocktail cOmplete™ (Sigma-Aldrich, St Louis, MO) in NativePAGE™ buffer (Invitrogen)). Extracted protein samples were centrifuged at 10000 g for 2 min and the supernatant was collected. After IP using the Dynabeads™ Protein G Immunoprecipitation Kit (1007D, Invitrogen), Western blots were prepared and probed using HRP-conjugated primary antibodies in 0.2% I-Block (T2015, Invitrogen). The antibodies used were F1804 (anti-FLAG, Sigma-Aldrich St Louis, MO, USA), A8592 (anti-FLAG-HRP, Sigma-Aldrich), H9658 (anti-HA, Sigma-Aldrich), 12013819001 (3F10, anti-HA-HRP, Roche, Basel, Switzerland), and SAB4700447 (anti-Myc, Sigma-Aldrich) at 1:5000 (v/v) dilutions. To detect ADP-ribosylated proteins, 1:5000 (v/v) dilution of an anti-ADPR reagent (MABE1016, EMD Millipore) was used with the anti-rabbit secondary antibody (A0545, Sigma-Aldrich). Proteins were visualized using the ECL Clarity or the ECL Clarity Max detection systems (Bio-Rad). The developed Western blots were rinsed with PBS and post-stained with Coomassie Brilliant Blue (CBB) to visualise protein bands for normalising protein loading.

Mass Spectrometry analysis

Four to five weeks old *N. benthamiana* leaves were syringe-infiltrated with a mixture of freshly grown Agrobacterium cultures of FLAG:AtRIN4 and AvrRpm1$_{Pma}$ (or AvrRpm2$_{Psa}$) in equal amounts (OD_{600}= 0.2 each) in the infiltration buffer (10 mM $MgCl_2$, 100 µM acetosyringone). At 2 d post infiltration, 1 g of infiltrated leaves were ground under liquid nitrogen to a fine powder. Two mL of extraction buffer (Pearce Co-IP buffer, Thermo-Fisher) was added to the ground tissues and the resulting suspension was thoroughly mixed. The suspended mix was left at room temperature for 30 min with agitation and then centrifuged at 10000 rpm for 2 min to collect the supernatant. A suspension of 100 µL of anti FLAG-conjugated magnetic beads (Pearce, Thermo-Fisher) was added to the collected fraction and the mixture was left at room temperature for 30 min with agitation. After this precipitation, the magnetic beads with immuno-precipitated proteins were collected and washed four times with PBS. 50 µL of SDS-PAGE sample buffer was added to the washed magnetic beads with attached proteins and the proteins were extracted from the magnetic

beads by heating the mix at 55°C for 12 min. The extracted proteins were run on a 4-12% SDS-PAGE gradient gel in MOPS running buffer. When the electrophoresis was completed, the gel was stained with Coomassie Brilliant Blue (CBB) and the visualised RIN4 protein bans was excised from the gel for mass spectrometry analysis.

Gel bands were destained, dehydrated with acetonitrile, and then subjected to reduction with 5 mM dithiothreitol, alkylation with 15 mM iodoacetamide, and digestion with 12.5 ng/µl modified sequencing grade porcine trypsin (Promega, Madison, WI) at 45°C for 1 hour. The digest was acidified with formic acid and then injected onto a 0.3×10 mm trap column packed with Reprosil C18 media (ESI Source Solutions, Woburn, MA) and desalted for 5 minutes at 10 µl/min before being separated on a 0.075 × 200 mm picofrit column (New Objective, Littleton, MA) packed with 3 µm Reprosil C18 media. The following gradient was applied at 300 nl/min using an Eksigent NanoLC 425 UPLC system (AB SCIEX, Concord, ON): 0 min 5% B; 20 min 40% B; 22 min 98% B; 24 min 98% B; 25 min 5% B; 30 min 5% B, where B was 0.1% formic acid in acetonitrile and the remainder of these solutions was solution A (0.1% formic acid in water). The picofrit spray was directed into a TripleTOF 6600 Quadrupole-Time-of-Flight mass spectrometer (AB SCIEX) scanning from 300-2000 m/z for 200ms, followed by 40ms MS/MS scans on the 35 most abundant multiply-charged peptides (m/z 80-1600). The mass spectrometer and HPLC system were under the control of the Analyst TF 1.8 software package (AB SCIEX). The resulting MS/MS data was searched against an in-house database comprising a set of common contaminant sequences, the FLAG-tagged Arabidopsis RIN4 sequence, plus *Nicotiana* and Rat entries from Uniprot.org (183,885 entries in total), using ProteinPilot version 5.0 (AB SCIEX). The peptide summary exported from ProteinPilot was further processed in Excel using a custom macro to remove proteins with Unused Scores below 1.3, eliminate inferior or redundant peptide spectral matches, and to sum the intensities for all unique peptides from each protein.

Accession numbers

Sequence data from this article can be found in the EMBL/GenBank data libraries under the following accession number(s): AtRIN4 (AT3G25070; NP_001325873), GmRIN4a (Glyma03g19920; NP_001235221), GmRIN4b (Glyma16g12160; NP_001239973), GmRIN4c (Glyma18g36000; NP_001235235), GmRIN4d

(Glyma08g46400; NP_001235252), PvRIN4a (XP_007134125.1), PvRIN4b (XP_007140654.1), MdRIN4-1(NM_001293994.1), MdRIN4-2 (NP_001280834.1), AvrB (WP_122390765.1), AvrRpm1$_{Pma}$ (NP_114197), AvrRpm2$_{Psa}$ (WP_099978761.1), RPM1 (At3g07040).

Primers used in this study

gAR2f1	CGCTATGACGTGATCGAGAA
gAR2r1	CAATACTGGCGTTGGAGTTC
AR2atgf1	ATGGGTAATATATGTGGTACTTC
AR2HAtgar1	TCAAGCGTAGTCTGGGACGTCGTATGGGTATCCGAAATCGTCGTCAGAATCT GACTGCA
gAR1f1	GAATTCGGCAAAAATCGTACGCAG
AR1atgf1	ATGGGCTGTGTATCGAGCAC
AR1taar1	TTAAAAGTCATCTTCTGAGTC
AR1HAtgar1	CTTATCTTAAGCGTAGTCTGGGACGTCGTATGGGTATCCAAAGTCATC TTCTGAGTCAGACTGAAC

SUPPLEMENTAL DATA

Fig S1. LC-MS/MS analysis of AtRIN4 co-expressed with AvrRpm1$_{Pma}$ in *N. benthamiana* via Agrobacterium.

Fig S2. Western blot analysis of modified RIN4 transiently co-expressed with AvrRpm1$_{Pma}$ in *N. benthamiana* via Agrobacterium.

Fig S3. LC-MS/MS analysis of AtRIN4 co-expressed with AvrRpm2$_{Psa}$ in *N. benthamiana* via Agrobacterium.

Fig S4. Western blot analysis of soybean RIN4 homologs modified by Pto DC3000Q^{-} (AvrRpm1$_{Pma}$).

COMPETING INTERESTS

The authors declare no conflict of interest.

ACKNOWLEDGEMENT

The authors thank Prof Andrew Allan and Dr Joanna Bowen of the New Zealand Institute for Plant and Food Research for critically reviewing the manuscript. This work was supported by the Plant and Food Research Fund KRIP PSA & RIN4 (P/880002/13). Further experimental details will be available upon request.

AUTHOR CONTRIBUTIONS

MY and ER conceived the study. MY designed and conducted experiments, and wrote the manuscript with input from all authors. MM conducted mass spectrometry analysis and wrote the mass spectrometry section in the Methods. ER acquired research funding, contributed to research through discussions, and edited the manuscript.

FIGURE LEGENDS

Figure 1. Transient co-expression of AtRIN4 and AvrRpm2$_{Psa}$ (biovar 5) in *N. benthamiana* via Agrobacterium. **A.** Sequence alignment of AvrRpm2$_{Psa}$ and AvrRpm1$_{Pma}$. The residues (H63, Y122, and D185) in the conserved H-Y-D motif of AvrRpm1$_{Pma,}$ proposed previously (Cherkis et al., 2012), are marked with blue labels. The corresponding residues in the H-Y-D motif of AvrRpm2$_{Psa}$ are H68, Y125, and D188**. B.** Western blot analysis demonstrating the ADP-ribosyl transferase activity of AvrRpm2$_{Psa}$. Proteins were extracted from *N. benthamiana* leaves co-expressing AvrRpm2$_{Psa}$:HA and FLAG:AtRIN4 via Agrobacterium at 2 d post infiltration. ADP-ribosylated proteins were detected using the anti ADPR binding reagent. FLAG:RIN4 and AvrRpm2$_{Psa}$:HA were detected using corresponding antibodies. **C**. RPM1-mediated HR (hypersensitive response) assay. An *N. benthamiana* leaf co-expressing FLAG:AtRIN4 and RPM1:Myc with either AvrRpm1$_{Pma}$ or AvrRpm1$_{Pma}$ in different combinations (1: AvrRpm1$_{Pma}^{WT}$:HA (wild type); 2: AvrRpm1$_{Pma}^{3A}$ (triple substitutions: H63A, Y122A, D185A); 3: AvrRpm2$_{Psa}^{WT}$:HA (wild type); 4: AvrRpm2$_{Psa}^{3A}$ (triple substitutions: H68A, Y125A, D188A) delivered via Agrobacterium. Red circles denote HR and white circles denote no HR. The fluorescence of the same leaf monitored under a 488 nm tray in the ChemiDoc™ is also shown (bottom). Images were taken 2 d post Agrobacterium

783 infiltration. **D**. Western blot analysis using proteins extracted from the corresponding areas of
784 the leaf used in **C** 2 d post Agrobacterium injection.

785 **Figure 2**. Western blot analysis of AtRIN4 transiently co-expressed with AvrRpm2$_{Psa}$ in *N.*
786 *benthamiana* via Agrobacterium. **A**. Proteins were extracted from *N. benthamiana* leaves co-
787 expressing FLAG:AtRIN4 with either Empty vector (lane 1), HA:AtRIN4 (lane 2), or
788 AvrRpm2$_{Psa}$:HA (lane 3) via Agrobacterium. Protein extracts were immunoprecipitated using
789 anti HA magnetic beads. Precipitated proteins were probed with corresponding antibodies. **B.**
790 Western blot analysis showed the ADP-ribosylated AtRIN4 migrated more slowly compared
791 with unmodified AtRIN4 during SDS-PAGE. Protein extracts from *N. benthamiana* leaves
792 co-expressing FLAG:AtRIN4 with AvrRpm2$_{Psa}$:HA (even-numbered) or expressing only
793 FLAG:AtRIN4 (odd-numbered) were probed. **C**. Western blot analysis of different
794 AvrRpm2$_{Psa}$ alelles (AvrRpm2$_{Psa}^{WT}$, AvrRpm2$_{Psa}^{H68A}$, AvrRpm2$_{Psa}^{Y125A}$, AvrRpm2$_{Psa}^{H188A}$,
795 and AvrRpm2$_{Psa}^{3A}$) co-expressed with AtRIN4 via Agrobacterium (Input panel). For Co-IP of
796 modified AvrRpm2 with AtRIN4 (Co-IP panels), protein extracts were precipitated using anti
797 FLAG magnetic beads to isolate FLAG:AtRIN4. Precipitated proteins were probed using
798 corresponding antibodies. **D.** Modified AvrRpm2 alleles (AvrRpm2$_{Psa}^{H68A}$, AvrRpm2$_{Psa}^{Y125A}$,
799 and AvrRpm2$_{Psa}^{D188A}$) were co-expressed with RPM1 and AtRIN4 on an *N. benthamiana* leaf
800 to assess the corresponding RPM1-mediated HR. **E.** Combinations of modified AvrRpm2
801 alleles (AvrRpm2$_{Psa}^{D188A}$ with AvrRpm2$_{Psa}^{H68A}$ and AvrRpm2$_{Psa}^{D188A}$ with AvrRpm2$_{Psa}^{Y125A}$)
802 were co-expressed with RPM1 and AtRIN4 on an *N. benthamiana* leaf. Red circles denote
803 HR and white circles denote no HR. Images were taken at 3 d post Agrobacterium injection
804 (**D** and **E**)

805 **Figure 3**. Secretion of bacterial effector via infection of Pto DC3000Q$^-$ in *N. benthamiana*. **A**.
806 An *N. benthamiana* leaf was infected with Pto DC3000Q$^-$(AvrRpm2$_{Psa}$) at a high
807 concentration (OD_{600}=1.0, or 5×10^8 cfu/mL) in the area pre-infiltrated with Agrobacterium 2
808 d earlier for transient expression of AtRIN4 (marked with a circle, bottom). Dark
809 discolouration and leaf margin malformations indicate Pto infection. The control area
810 infiltrated only with Agrobacterium is also marked (top). Image was taken at 15 h post
811 infection. **B**. Western blot analysis demonstrated that AtRIN4 was ADP-ribosylated upon
812 infection with Pto DC3000Q$^-$(AvrRpm2$_{Psa}$). Proteins were extracted from *N. benthamiana*
813 leaves expressing AtRIN4 via Agrobacterium after infection with Pto DC3000Q$^-$
814 (AvrRpm2$_{Psa}$). ADP-ribosylated proteins were detected using anti ADPR binding reagent.

(EV: control Pto DC3000Q$^-$ with an empty vector). **C**. Alignment of the two NOI sequences in RIN4 homologs of Arabidopsis (AtRIN4), snap bean (PvRIN4a and PvRIN4b) and soybean (GmRIN4a to GmRIN4d). **D**. Western blot analysis of RIN4 co-expressed with AvrRpm2$_{Psa}$ *in planta* via Agrobacterium. **E**. Western blot analysis of RIN4 homologs infected with Pto DC3000Q$^-$(AvrRpm2$_{Psa}$). Proteins were extracted as in (**B**). **F**. The indicated RIN4 homologs were co-expressed with AvrRpm2$_{Psa}$ and RPM1 in different areas of an *N. benthamiana* leaf via Agrobacterium to assess the corresponding RPM1-mediated HR. Red circles denote HR and white circles denote no HR.

Figure 4. Identification of the target residue for AvrRpm2$_{Psa}$ by mutational analysis. **A**. Modifications generated in the two NOI sequences of AtRIN4. The ten modifications (N11A, E13A, E15A, E16A, N17A, D153A, D155A, E156A, N157A, N158A) in AtRIN4^{10A} are boxed in black ( ) and the six modifications in AtRIN4^{6A} (N11A, E16A, N17D, D153A, N157A, N158A) are marked with asterisk (* in N11 and D153, previously identified by Redditt et al.) (Redditt et al., 2019) or closed circle (• in E16, N17, N157, and N158 identified in this study). **B**. Western blot analysis of RIN4 proteins (AtRIN4^{WT}, GmRIN4b^{WT}, AtRIN4^{6A} and AtRIN4^{10A}) from leaves infected with with Pto DC3000Q$^-$(AvrRpm2$_{Psa}$). Proteins were extracted 1 d post infection of Pto DC3000Q$^-$(AvrRpm2) in *N. benthamiana* leaves pre-infiltrated with Agrobacterium 2 d earlier for transient expression of RIN4. **C**. AtRIN4^{10A} was co-expressed with AvrRpm2$_{Psa}$ and RPM1 in *N. benthamiana* to assess the RPM1-mediated HR. HR was assessed visually (left) or by monitoring fluorescence with ChemiDoc™ (right) at 2 d post Agrobacterium infiltration. **D**. Western blot analysis of the five AtRIN4^{8A} variant proteins (AtRIN4$^{8A}_{E11D153}$, AtRIN4$^{8A}_{E13D155}$, AtRIN4$^{8A}_{E15E156}$, AtRIN4$^{8A}_{E16N157}$, and AtRIN4$^{8A}_{N17N158}$) from leaves infected with with Pto DC3000Q$^-$ (AvrRpm2$_{Psa}$). Proteins were extracted as in (**B**). **E**. The five AtRIN4^{8A} proteins were co-expressed with AvrRpm2$_{Psa}$ and RPM1 in *N. benthamiana* via Agrobacterium to assess the corresponding HR. Visual inspection (left) and fluorescence test using the ChemiDoc™ (right) are shown. **F**. Western blot analysis of AtRIN4 proteins (AtRIN4^{WT}, AtRIN4^{E15AE156A}, AtRIN4^{E15A}, and AtRIN4^{E156A}) from leaves infected with Pto DC3000Q$^-$(AvrRpm2$_{Psa}$). Proteins were extracted as in (**B**). **G**. AtRIN4 proteins (AtRIN4^{WT}, AtRIN4^{E15AE156A}, AtRIN4^{E15A}, and AtRIN4^{E156A}) were co-expressed with AvrRpm2$_{Psa}$ and RPM1 in *N. benthamiana* to assess the RPM1-mediated HR. The visual inspection (left) and the fluorescence test with the ChemiDoc™ (right) are shown. Red circles denote HR and white circles denote no HR.

Figure 5. Western blot analysis of soybean RIN4 homologs from *N. benthamiana* leaves infected with Pto DC3000Q$^-$(AvrRpm2$_{Psa}$). **A**. Sequence alignment of the nitrate-induced (NOI) sequences in RIN4 homologs of Arabidopsis (AtRIN4) and soybean (GmRIN4a, GmRIN4b, GmRIN4c, and GmRIN4d). E156 in AtRIN4 corresponds to E189 in GmRIN4c or E180 in GmRIN4d, respectively. GmRIN4a and GmRIN4b have a valine (V) at the corresponding positions. **B**. Western blot analysis of soybean RIN4 homologs after infection with Pto DC3000Q$^-$(AvrRpm2$_{Psa}$). Proteins were extracted from *N. benthamiana* leaves 1 d post infiltration of Pto DC3000Q$^-$(AvrRpm2$_{Psa}$) following Agrobacterium infiltration 2 d earlier for transient expression RIN4 homologs. **C**. Soybean RIN4 homologs were co-expressed with AvrRpm2$_{Psa}$ and RPM1 in *N. benthamiana* via Agrobacterium to assess the RPM1-mediated HR. The visual image was taken in 4 d post Agrobacterium infiltration. Red circles denote HR and white circles denote no HR. **D**. Western blot analysis of GmRIN4c^{E189A} and GmRIN4d^{E180A} from *N. benthamiana* leaves infected with Pto DC3000Q$^-$ (AvrRpm2$_{Psa}$). Proteins extraction and Western blot analysis were performed as in (**B**). **E**. Western blot analysis of GmRIN4b^{V188E} and GmRIN4b^{G16E} from *N. benthamiana* leaves infected with Pto DC3000Q$^-$(AvrRpm2$_{Psa}$). Proteins extraction and Western blot analysis were performed as in (**B**).

Figure 6. Western blot analysis and RPM1-mediated HR assay of apple RIN4 homologs. **A**. Sequence alignment of the NOI sequences in the RIN4 homologs of Arabidopsis (AtRIN4), snap bean (PvRIN4a and PvRIN4b), soybean (GmRIN4a to GmRIN4d), and apple (MdRIN4-1 and MdRIN4-2). Both apple RIN4 loci have glutamate residues at the positions (E186 in MdRIN4-2 and E184 in MdRIN4-1) corresponding to E156 of AtRIN4. MdRIN4-2 also has a glutamate (E16) at the position corresponding to E15 of AtRIN4, while MdRIN4-1 has an alternative residue glutamine (Q16). **B**. Western blot analysis of MdRIN4-2^{E186A} (left). Proteins were extracted 1 d post infection of Pto DC3000Q$^-$(AvrRpm2$_{Psa}$) into *N. benthamiana* leaves pre-infiltrated with Agrobacterium 2 d earlier for transient expression of RIN4 homologs. Apple RIN4 homologs were co-expressed with AvrRpm2$_{Psa}$ and RPM1 in *N. benthamiana* via Agrobacterium to assess the RPM1-mediated HR (right). **C**. Western blot analysis of MdRIN4-1^{Q16E} with other RIN4 homologs (left). Protein extractions and Western blot analysis were performed as in (**B**). MdRIN4-1^{Q16E} and other RIN4 homologs were co-expressed with AvrRpm2$_{Psa}$ and RPM1 via Agrobacterium in different areas of an *N. benthamiana* leaf to assess the RPM1-mediated HR.

Figure 7. Activities of the type three effectors (T3Es) triggering RPM1 activation. **A**. Western blot analysis of RIN4 homologs of Arabidopsis (AtRIN4) and soybean (GmRIIN4a to GmRIN4d) co-expressed in *N. benthamiana* via Agrobacterium. Proteins were extracted from *N. benthamiana* leaves co-expressing AvrB with RIN4 via Agrobacterium at 2 d post infiltration. **B**. Different AtRIN4 alleles ($AtRIN4^{WT}$, $AtRIN4^{E156A}$ or $AtRIN4^{T21AS1690AT166A}$) and RPM1 were co-expressed with either $AvrRpm2_{Psa}$ (left half) or AvrB (right half) on an *N. benthamiana* leaf via Agrobacterium to assess the corresponding RPM1-mediated HR. **C**. Western blot analysis of different AtRIN4 alleles ($AtRIN4^{WT}$, $AtRIN4^{E156A}$, $AtRIN4^{T21A}$, $AtRIN4^{T166A}$, $AtRIN4^{T21AT166A}$, and $AtRIN4^{T21AS1690AT166A}$) from *N. benthamiana* leaves infected with Pto DC3000Q$^-$($AvrRpm2_{Psa}$) (left). Proteins were extracted 1 d post infection of Pto DC3000Q$^-$($AvrRpm2_{Psa}$) into *N. benthamiana* leaves pre-infiltrated with Agrobacterium 2 d earlier for transient expression of the RIN4 alleles. The AtRIN4 alleles were co-expressed with $AvrRpm2_{Psa}$ and RPM1 on different areas of an *N. benthamiana* leaf via Agrobacterium (right). **D**. Western blot analysis of $AtRIN4^{E156A}$ from *N. benthamiana* leaves infected with either Pto DC3000Q$^-$($AvrRpm2_{Psa}$) or by Pto DC3000Q$^-$($AvrRpm1_{Pma}$) (left). $AtRIN4^{E156A}$ and RPM1 were co-expressed with either $AvrRpm2_{Psa}$ or $AvrRpm1_{Pma}$ on different areas of an *N. benthamiana* leaf to assess the RPM1-mediated HR (right). Red circles denote HR and white circles denote no HR.

Figure 8. Activity and physical association of $AvrRpm2_{Psa}$ alleles. **A**. Sequence alignment of $AvrRpm2_{Psa}$ alleles from different Psa biovars. The biovar1 and biovar3 alleles were edited to express corresponding full-length proteins by removing extra nucleotides. The corrected sites are marked in black. The two residues H68 and Y125 are marked in blue and D188 is in green. All other substitutions are marked in red. **B**. Western blot analysis of AtRIN4 co-expressed with different $AvrRpm2_{Psa}$ alleles (input panel). Proteins were extracted 2 d after co-infiltration of AtRIN4 and $AvrRpm2_{Psa}$ in *N. benthamiana* via Agrobacterium. Co-IP of AtRIN4 with different $AvrRpm2_{Psa}$ proteins (Co-IP panel). Proteins were immunoprecipitated using anti FLAG magnetic beads to isolate AtRIN4. The precipitated proteins were probed using corresponding antibodies. **C**. $AvrRpm2_{Psa}$ alleles from different Psa biovars were co-expressed with AtRIN4 and RPM1 via Agrobacterium on different areas of an *N. benthamiana* leaf to assess the RPM1-mediated HR. Red circles denote HR, white circles denote no HR, and orange circle denotes reduced HR. Visual inspection (left) and fluorescence detection monitored in the ChemiDoc™ system (right) were shown.

Supplemental Data

Figure S1. LC-MS/MS analysis of AtRIN4 co-expressed with AvrRpm1$_{Pma}$ in *N. benthamiana* via agrobacterium. **A**. A Coomassie Brilliant Blue (CBB) stained SDS-PAGE gel after immunoprecitation of protein extracts from *N. benthamiana* leaves co-infiltrated with FLAGA:AtRIN4 and AvrRpm1$_{Pma}$ via agrobacterium (EV: empty vector). **B**. Confirmation of excised FLAG:AtRIN4 by Western blot analysis using anti FLAG antibody. FLAG:AtRIN4 band was excised from the gel and boiled in 2× sampling buffer for 5 min (IP). **C**. Summary of fragment ions in the LC-MS/MS spectra of the modified AtRIN4 peptides (not all fragmentations are shown). ADP-ribose moieties were identified at N157, N158, and N17. Fragmentation evidence also suggested that either E15 or E16 was modified in one peptide (top). **D.** An example of LC-MS/MS fragmentation evidence, showing N17 was modified with a ribose derived from ADP-ribose. (ADP-R: ADP-ribose, P-R: phospho-ribose, R: ribose, y: y-ions, b: b-ions).

Figure S2. Western blot analysis of modified RIN4 transiently co-expressed with AvrRpm1$_{Pma}$ in *N. benthamiana* via Agrobacterium. **A**. Western blot of proteins extracted form *N. benthamiana* leaves co-expressing AvrRpm1$_{Pma}$ with GmRIN4b^{N12AD185A} or AtRIN4^{N11AD153A}, modified based on previous mass spectrometry analyses (Redditt et al., 2019), via agrobacterium. **B**. Western blot of proteins extracted form *N. benthamiana* leaves co-expressing AvrRpm1$_{Pma}$ with AtRIN4^{E16AN17AN157AN158A}, modified based on our mass spectrometry analysis, or AtRIN4^{E11AE16AN17AD153N157AN158A}, with all collectively identified residues blocked, via agrobacterium. **C**. Modified RIN4 homologs (GmRIN4b^{N12AD185A}, AtRIN4^{N11AD153A}, and AtRIN4^{E16AN17AN157AN158A}) and unmodified RIN4 homologs (AtRIN4^{WT} and GmRIN4b^{WT}) were co-expressed with RPM1 and AvrRpm1$_{Pma}$ in *N. benthamiana* via agrobacterium. YFP was also co-expressed with RPM1 and AvrRpm1$_{Pma}$ as a negative control for RPM1-mediated response. Red circles denote HR and white circle denotes no HR.

Figure S3. LC-MS/MS analysis of AtRIN4 co-expressed with AvrRpm2$_{Psa}$ in *N. benthamiana* via agrobacterium. **A**. Summary of fragment ions in the LC-MS/MS spectra of the modified AtRIN4 peptides. The locations of the targets predicted from the LC-MS/MS fragmentation are marked with blue boxes. Identified ADP-ribose moieties are labelled in

orange. **B**. An example of fragmentation evidence suggesting the target site is either D155, E156, N157, or N158 in this peptide. (ADP-R: ADP-ribose, R: ribose, y: y-ions, b: b-ions).

Figure S4. Western blot analysis of soybean RIN4 homologs modified by Pto DC3000Q$^-$ (AvrRpm1$_{Pma}$). Proteins were extracted from *N. benthamiana* leaves infected with Pto DC3000Q$^-$(AvrRpm1$_{Pma}$) in 1 d post infection, following Agrobacterium infiltration 2 d earlier for transient expression of RIN4 homologs.

Parsed Citations

Abelleira, A., Ares, A., Aguin, O., Penalver, J., Morente, M.C., Lopez, M.M., Sainz, M.J., and Mansilla, J.P. (2015). Detection and characterization of Pseudomonas syringae pv. actinidifoliorum in kiwifruit in Spain. J Appl Microbiol 119, 1659-1671.
Google Scholar: Author Only Title Only Author and Title

Afzal, A.J., Kim, J.H., and Mackey, D. (2013). The role of NOI-domain containing proteins in plant immune signaling. BMC Genomics 14, 327.
Google Scholar: Author Only Title Only Author and Title

Alfano, J.R., and Collmer, A. (2004). Type III secretion system effector proteins: double agents in bacterial disease and plant defense. Annu Rev Phytopathol 42, 385-414.
Google Scholar: Author Only Title Only Author and Title

Ausubel, F.M. (2005). Are innate immune signaling pathways in plants and animals conserved? Nat Immunol 6, 973-979.
Google Scholar: Author Only Title Only Author and Title

Baltrus, D.A., Nishimura, M.T., Romanchuk, A., Chang, J.H., Mukhtar, M.S., Cherkis, K., Roach, J., Grant, S.R., Jones, C.D., and Dangl, J.L. (2011). Dynamic evolution of pathogenicity revealed by sequencing and comparative genomics of 19 Pseudomonas syringae isolates. PLoS Pathog 7, e1002132.
Google Scholar: Author Only Title Only Author and Title

Belkhadir, Y., Subramaniam, R., and Dangl, J.L. (2004). Plant disease resistance protein signaling: NBS-LRR proteins and their partners. Current Opinion in Plant Biology 7, 391-399.
Google Scholar: Author Only Title Only Author and Title

Bent, A.F., and Mackey, D. (2007). Elicitors, effectors, and R genes: The new paradigm and a lifetime supply of questions. Annual Review of Phytopathology 45, 399-436.
Google Scholar: Author Only Title Only Author and Title

Block, A., and Alfano, J.R. (2011). Plant targets for Pseudomonas syringae type III effectors: virulence targets or guarded decoys? Curr Opin Microbiol 14, 39-46.
Google Scholar: Author Only Title Only Author and Title

Block, A., Li, G., Fu, Z.Q., and Alfano, J.R. (2008). Phytopathogen type III effector weaponry and their plant targets. Curr Opin Plant Biol 11, 396-403.
Google Scholar: Author Only Title Only Author and Title

Buscaill, P., Sanguankiattichai, N., Lee, Y.J., Kourelis, J., Preston, G., and van der Hoorn, R.A.L. (2021). Agromonas: a rapid disease assay for Pseudomonas syringae growth in agroinfiltrated leaves. Plant J 105, 831-840.
Google Scholar: Author Only Title Only Author and Title

Buttner, D. (2012). Protein export according to schedule: architecture, assembly, and regulation of type III secretion systems from plant- and animal-pathogenic bacteria. Microbiol Mol Biol Rev 76, 262-310.
Google Scholar: Author Only Title Only Author and Title

Cherkis, K.A., Temple, B.R., Chung, E.H., Sondek, J., and Dangl, J.L. (2012). AvrRpm1 missense mutations weakly activate RPS2-mediated immune response in Arabidopsis thaliana. PLoS One 7, e42633.
Google Scholar: Author Only Title Only Author and Title

Chung, E.H., El-Kasmi, F., He, Y., Loehr, A., and Dangl, J.L. (2014). A plant phosphoswitch platform repeatedly targeted by type III effector proteins regulates the output of both tiers of plant immune receptors. Cell Host Microbe 16, 484-494.
Google Scholar: Author Only Title Only Author and Title

Chung, E.H., da Cunha, L., Wu, A.J., Gao, Z., Cherkis, K., Afzal, A.J., Mackey, D., and Dangl, J.L. (2011). Specific threonine phosphorylation of a host target by two unrelated type III effectors activates a host innate immune receptor in plants. Cell Host Microbe 9, 125-136.
Google Scholar: Author Only Title Only Author and Title

Cohen, M.S., and Chang, P. (2018). Insights into the biogenesis, function, and regulation of ADP-ribosylation. Nat Chem Biol 14, 236-243.
Google Scholar: Author Only Title Only Author and Title

Coombes, B.K. (2009). Type III secretion systems in symbiotic adaptation of pathogenic and non-pathogenic bacteria. Trends Microbiol 17, 89-94.
Google Scholar: Author Only Title Only Author and Title

Cui, H., Tsuda, K., and Parker, J.E. (2015). Effector-triggered immunity: from pathogen perception to robust defense. Annu Rev Plant Biol 66, 487-511.
Google Scholar: Author Only Title Only Author and Title

Cunnac, S., Lindeberg, M., and Collmer, A. (2009). Pseudomonas syringae type III secretion system effectors: repertoires in search of functions. Current Opinion in Microbiology 12, 53-60.

Google Scholar: Author Only Title Only Author and Title

Dangl, J.L., and Jones, J.D. (2001). Plant pathogens and integrated defence responses to infection. Nature 411, 826-833.
Google Scholar: Author Only Title Only Author and Title

DeYoung, B.J., and Innes, R.W. (2006). Plant NBS-LRR proteins in pathogen sensing and host defense. Nat Immunol 7, 1243-1249.
Google Scholar: Author Only Title Only Author and Title

Dharmaraj, K. (2018). Functional characterization of Pseudomonas syringae pv. actinidiae effectors AvrPto5 and HopF2 (New Zealand: The University of Auckland).
Google Scholar: Author Only Title Only Author and Title

Dodds, P.N., and Rathjen, J.P. (2010). Plant immunity: towards an integrated view of plant-pathogen interactions. Nat Rev Genet 11, 539-548.
Google Scholar: Author Only Title Only Author and Title

Doll, S., and Burlingame, A.L. (2015). Mass spectrometry-based detection and assignment of protein posttranslational modifications. ACS Chem Biol 10, 63-71.
Google Scholar: Author Only Title Only Author and Title

Donati, I., Cellini, A., Sangiorgio, D., Vanneste, J.L., Scortichini, M., Balestra, G.M., and Spinelli, F. (2020). Pseudomonas syringae pv. actinidiae: Ecology, Infection Dynamics and Disease Epidemiology. Microb Ecol 80, 81-102.
Google Scholar: Author Only Title Only Author and Title

Fang, Y., Zhu, X., and Wang, Y. (1990). Preliminary studies on kiwifruit diseases in Hunan province. . Sichuan Fruit Science and Technology 18, 28–29.
Google Scholar: Author Only Title Only Author and Title

Felix, G., Duran, J.D., Volko, S., and Boller, T. (1999). Plants have a sensitive perception system for the most conserved domain of bacterial flagellin. Plant J 18, 265-276.
Google Scholar: Author Only Title Only Author and Title

Feng, B., Liu, C., Shan, L., and He, P. (2016). Protein ADP-Ribosylation Takes Control in Plant-Bacterium Interactions. PLoS Pathog 12, e1005941.
Google Scholar: Author Only Title Only Author and Title

Fujikawa, T., and Sawada, H. (2016). Genome analysis of the kiwifruit canker pathogen Pseudomonas syringae pv. actinidiae biovar 5. Sci Rep 6, 21399.
Google Scholar: Author Only Title Only Author and Title

Fujikawa, T., and Sawada, H. (2019). Genome analysis of Pseudomonas syringae pv. actinidiae biovar 6, which produces the phytotoxins, phaseolotoxin and coronatine. Sci Rep 9, 3836.
Google Scholar: Author Only Title Only Author and Title

Garrity-Ryan, L., Shafikhani, S., Balachandran, P., Nguyen, L., Oza, J., Jakobsen, T., Sargent, J., Fang, X., Cordwell, S., Matthay, M.A., and Engel, J.N. (2004). The ADP ribosyltransferase domain of Pseudomonas aeruginosa ExoT contributes to its biological activities. Infect Immun 72, 546-558.
Google Scholar: Author Only Title Only Author and Title

Guo, M., Tian, F., Wamboldt, Y., and Alfano, J.R. (2009). The Majority of the Type III Effector Inventory of Pseudomonas syringae pv. tomato DC3000 Can Suppress Plant Immunity. Mol Plant Microbe In 22, 1069-1080.
Google Scholar: Author Only Title Only Author and Title

Hendriks, I.A., Larsen, S.C., and Nielsen, M.L. (2019). An Advanced Strategy for Comprehensive Profiling of ADP-ribosylation Sites Using Mass Spectrometry-based Proteomics. Mol Cell Proteomics 18, 1010-1026.
Google Scholar: Author Only Title Only Author and Title

Hottiger, M.O., Hassa, P.O., Luscher, B., Schuler, H., and Koch-Nolte, F. (2010). Toward a unified nomenclature for mammalian ADP-ribosyltransferases. Trends Biochem Sci 35, 208-219.
Google Scholar: Author Only Title Only Author and Title

Ingle, R.A., Carstens, M., and Denby, K.J. (2006). PAMP recognition and the plant-pathogen arms race. Bioessays 28, 880-889.
Google Scholar: Author Only Title Only Author and Title

Kim, M.G., da Cunha, L., McFall, A.J., Belkhadir, Y., DebRoy, S., Dangl, J.L., and Mackey, D. (2005). Two Pseudomonas syringae type III effectors inhibit RIN4-regulated basal defense in Arabidopsis. Cell 121, 749-759.
Google Scholar: Author Only Title Only Author and Title

Koh, Y., Cha, B., Chung, H., and Lee, D. (1994). Outbreak and spread of bacterial canker in kiwifruit. Korean Journal of Plant Pathology 10, 68–72.
Google Scholar: Author Only Title Only Author and Title

Kong, L., Rodrigues, B., Kim, J.H., He, P., and Shan, L. (2021). More than an on-and-off switch: Post-translational modifications of plant pattern recognition receptor complexes. Curr Opin Plant Biol 63, 102051.

Google Scholar: Author Only Title Only Author and Title

Lee, C.C., Wood, M.D., Ng, K., Andersen, C.B., Liu, Y., Luginbuhl, P., Spraggon, G., and Katagiri, F. (2004). Crystal structure of the type III effector AvrB from Pseudomonas syringae. Structure 12, 487-494.
Google Scholar: Author Only Title Only Author and Title

Lee, D., Bourdais, G., Yu, G., Robatzek, S., and Coaker, G. (2015a). Phosphorylation of the Plant Immune Regulator RPM1-INTERACTING PROTEIN4 Enhances Plant Plasma Membrane H(+)-ATPase Activity and Inhibits Flagellin-Triggered Immune Responses in Arabidopsis. Plant Cell 27, 2042-2056.
Google Scholar: Author Only Title Only Author and Title

Lee, J., Manning, A.J., Wolfgeher, D., Jelenska, J., Cavanaugh, K.A., Xu, H., Fernandez, S.M., Michelmore, R.W., Kron, S.J., and Greenberg, J.T. (2015b). Acetylation of an NB-LRR Plant Immune-Effector Complex Suppresses Immunity. Cell Rep 13, 1670-1682.
Google Scholar: Author Only Title Only Author and Title

Lindeberg, M., Cunnac, S., and Collmer, A. (2012). Pseudomonas syringae type III effector repertoires: last words in endless arguments. Trends Microbiol 20, 199-208.
Google Scholar: Author Only Title Only Author and Title

Liu, J., Elmore, J.M., Lin, Z.J., and Coaker, G. (2011). A receptor-like cytoplasmic kinase phosphorylates the host target RIN4, leading to the activation of a plant innate immune receptor. Cell Host Microbe 9, 137-146.
Google Scholar: Author Only Title Only Author and Title

Macho, A.P., and Zipfel, C. (2015). Targeting of plant pattern recognition receptor-triggered immunity by bacterial type-III secretion system effectors. Curr Opin Microbiol 23, 14-22.
Google Scholar: Author Only Title Only Author and Title

Mackey, D., Holt, B.F., 3rd, Wiig, A., and Dangl, J.L. (2002). RIN4 interacts with Pseudomonas syringae type III effector molecules and is required for RPM1-mediated resistance in Arabidopsis. Cell 108, 743-754.
Google Scholar: Author Only Title Only Author and Title

Mackey, D., Belkhadir, Y., Alonso, J.M., Ecker, J.R., and Dangl, J.L. (2003). Arabidopsis RIN4 is a target of the type III virulence effector AvrRpt2 and modulates RPS2-mediated resistance. Cell 112, 379-389.
Google Scholar: Author Only Title Only Author and Title

Malinovsky, F.G., Fangel, J.U., and Willats, W.G. (2014). The role of the cell wall in plant immunity. Front Plant Sci 5, 178.
Google Scholar: Author Only Title Only Author and Title

Mansfield, J., Genin, S., Magori, S., Citovsky, V., Sriariyanum, M., Ronald, P., Dow, M., Verdier, V., Beer, S.V., Machado, M.A., Toth, I., Salmond, G., and Foster, G.D. (2012). Top 10 plant pathogenic bacteria in molecular plant pathology. Mol Plant Pathol 13, 614-629.
Google Scholar: Author Only Title Only Author and Title

McCann, H.C., Li, L., Liu, Y., Li, D., Pan, H., Zhong, C., Rikkerink, E.H.A., Templeton, M.D., Straub, C., Colombi, E., Rainey, P.B., and Huang, H. (2017). Origin and Evolution of the Kiwifruit Canker Pandemic. Genome Biol Evol 9, 932-944.
Google Scholar: Author Only Title Only Author and Title

McCann, H.C., Rikkerink, E.H., Bertels, F., Fiers, M., Lu, A., Rees-George, J., Andersen, M.T., Gleave, A.P., Haubold, B., Wohlers, M.W., Guttman, D.S., Wang, P.W., Straub, C., Vanneste, J.L., Rainey, P.B., and Templeton, M.D. (2013). Genomic analysis of the Kiwifruit pathogen Pseudomonas syringae pv. actinidiae provides insight into the origins of an emergent plant disease. PLoS Pathog 9, e1003503.
Google Scholar: Author Only Title Only Author and Title

Mikolcevic, P., Hlousek-Kasun, A., Ahel, I., and Mikoc, A. (2021). ADP-ribosylation systems in bacteria and viruses. Comput Struct Biotechnol J 19, 2366-2383.
Google Scholar: Author Only Title Only Author and Title

Puhar, A., and Sansonetti, P.J. (2014). Type III secretion system. Curr Biol 24, R784-791.
Google Scholar: Author Only Title Only Author and Title

Ray, S.K., Macoy, D.M., Kim, W.Y., Lee, S.Y., and Kim, M.G. (2019). Role of RIN4 in Regulating PAMP-Triggered Immunity and Effector-Triggered Immunity: Current Status and Future Perspectives. Mol Cells 42, 503-511.
Google Scholar: Author Only Title Only Author and Title

Redditt, T.J., Chung, E.H., Karimi, H.Z., Rodibaugh, N., Zhang, Y., Trinidad, J.C., Kim, J.H., Zhou, Q., Shen, M., Dangl, J.L., Mackey, D., and Innes, R.W. (2019). AvrRpm1 Functions as an ADP-Ribosyl Transferase to Modify NOI Domain-Containing Proteins, Including Arabidopsis and Soybean RPM1-Interacting Protein4. Plant Cell 31, 2664-2681.
Google Scholar: Author Only Title Only Author and Title

Ribet, D., and Cossart, P. (2010). Post-translational modifications in host cells during bacterial infection. Febs Letters 584, 2748-2758.
Google Scholar: Author Only Title Only Author and Title

Rikkerink, E.H.A. (2018). Pathogens and Disease Play Havoc on the Host Epiproteome-The "First Line of Response" Role for Proteomic Changes Influenced by Disorder. Int J Mol Sci 19.
Google Scholar: Author Only Title Only Author and Title

Rosenthal, F., Nanni, P., Barkow-Oesterreicher, S., and Hottiger, M.O. (2015). Optimization of LTQ-Orbitrap Mass Spectrometer Parameters for the Identification of ADP-Ribosylation Sites. J Proteome Res 14, 4072-4079.
Google Scholar: Author Only Title Only Author and Title

Scortichini, M. (1994). Occurrence of Pseudomonas syringae pv. actinidiae on Kiwifruit in Italy. Plant Pathol 43, 1035–1038.
Google Scholar: Author Only Title Only Author and Title

Serizawa, S., Ichikawa, T., Takikawa, Y., Tsuyumu, S., and Goto, M. (1989). Occurrence of bacterial canker of kiwifruit in Japan: description of symptoms, isolation of the pathogen and screening of bactericides. Annals of the Phytopathological Society of Japan 55, 427-436
Google Scholar: Author Only Title Only Author and Title

Simon, N.C., Aktories, K., and Barbieri, J.T. (2014). Novel bacterial ADP-ribosylating toxins: structure and function. Nat Rev Microbiol 12, 599-611.
Google Scholar: Author Only Title Only Author and Title

Sun, X., Greenwood, D.R., Templeton, M.D., Libich, D.S., McGhie, T.K., Xue, B., Yoon, M., Cui, W., Kirk, C.A., Jones, W.T., Uversky, V.N., and Rikkerink, E.H. (2014). The intrinsically disordered structural platform of the plant defence hub protein RPM1-interacting protein 4 provides insights into its mode of action in the host-pathogen interface and evolution of the nitrate-induced domain protein family. FEBS J 281, 3955-3979.
Google Scholar: Author Only Title Only Author and Title

Toruno, T.Y., Shen, M., Coaker, G., and Mackey, D. (2019). Regulated Disorder: Posttranslational Modifications Control the RIN4 Plant Immune Signaling Hub. Mol Plant Microbe Interact 32, 56-64.
Google Scholar: Author Only Title Only Author and Title

van der Hoorn, R.A., and Kamoun, S. (2008). From Guard to Decoy: a new model for perception of plant pathogen effectors. Plant Cell 20, 2009-2017.
Google Scholar: Author Only Title Only Author and Title

Vanneste, J.L., Yu, J., Cornish, D.A., Tanner, D.J., Windner, R., Chapman, J.R., Taylor, R.K., Mackay, J.F., and Dowlut, S. (2013). Identification, Virulence, and Distribution of Two Biovars of Pseudomonas syringae pv. actinidiae in New Zealand. Plant Dis 97, 708-719.
Google Scholar: Author Only Title Only Author and Title

Wei, C.F., Kvitko, B.H., Shimizu, R., Crabill, E., Alfano, J.R., Lin, N.C., Martin, G.B., Huang, H.C., and Collmer, A. (2007). A Pseudomonas syringae pv. tomato DC3000 mutant lacking the type III effector HopQ1-1 is able to cause disease in the model plant Nicotiana benthamiana. Plant J 51, 32-46.
Google Scholar: Author Only Title Only Author and Title

Wilton, M., Subramaniam, R., Elmore, J., Felsensteiner, C., Coaker, G., and Desveaux, D. (2010). The type III effector HopF2Pto targets Arabidopsis RIN4 protein to promote Pseudomonas syringae virulence. Proc Natl Acad Sci U S A 107, 2349-2354.
Google Scholar: Author Only Title Only Author and Title

Xu, N., Luo, X., Li, W., Wang, Z., and Liu, J. (2017). The Bacterial Effector AvrB-Induced RIN4 Hyperphosphorylation Is Mediated by a Receptor-Like Cytoplasmic Kinase Complex in Arabidopsis. Mol Plant Microbe Interact 30, 502-512.
Google Scholar: Author Only Title Only Author and Title

Yoon, M., and Rikkerink, E.H.A. (2020). Rpa1 mediates an immune response to avrRpm1Psa and confers resistance against Pseudomonas syringae pv. actinidiae. Plant J 102, 688-702.
Google Scholar: Author Only Title Only Author and Title

Yu, T.Y., Sun, M.K., and Liang, L.K. (2021). Receptors in the Induction of the Plant Innate Immunity. Mol Plant Microbe Interact, MPMI07200173CR.
Google Scholar: Author Only Title Only Author and Title

Zhao, G., Guo, D., Wang, L., Li, H., Wang, C., and Guo, X. (2021). Functions of RPM1-interacting protein 4 in plant immunity. Planta 253, 11.
Google Scholar: Author Only Title Only Author and Title